

NIST Technical Note 1920

**Predicting the Effects of
Barrier Fabrics on
Residential Upholstered
Furniture Fire Hazard**

Morgan C. Bruns

This publication is available free of charge from:
<http://dx.doi.org/10.6028/NIST.TN.1920>

NIST Technical Note 1920

Predicting the Effects of Barrier Fabrics on Residential Upholstered Furniture Fire Hazard

Morgan C. Bruns
*Fire Research Division
Engineering Laboratory*

This publication is available free of charge from:
<http://dx.doi.org/10.6028/NIST.TN.1920>

June 2016



U.S. Department of Commerce
Penny Pritzker, Secretary

National Institute of Standards and Technology
Willie May, Under Secretary of Commerce for Standards and Technology and Acting Director

Certain commercial entities, equipment, or materials may be identified in this document in order to describe an experimental procedure or concept adequately. Such identification is not intended to imply recommendation or endorsement by the National Institute of Standards and Technology, nor is it intended to imply that the entities, materials, or equipment are necessarily the best available for the purpose.

National Institute of Standards and Technology Technical Note 1920
Natl. Inst. Stand. Technol. Tech. Note 1920, 46 pages (June 2016)
CODEN: NTNOEF

This publication is available free of charge from:
<http://dx.doi.org/10.6028/NIST.TN.1920>

Contents

Contents	iii
List of Figures	iv
List of Tables	v
List of Acronyms	vi
List of Symbols	vii
1 Introduction	1
1.1 Objective and Technical Approach	1
1.2 Literature Review	2
1.3 Outline of Report	4
2 Predicting Fire Losses	5
2.1 Models for Fire Losses	5
2.2 Estimating Fire Loss Probabilities	6
3 Data	8
3.1 Overview	8
3.2 Chair Fire Data	8
3.3 Building Statistics	12
4 Model Descriptions	20
4.1 Overview and Selection of Loss Metrics	20
4.2 Empirical Correlation	21
4.3 Zone Model	23
5 Results	27
5.1 Overview	27
5.2 Predicting Hazard with the MQH Correlation	28
5.2.1 Inverse MQH	28
5.2.2 Forward MQH	32
5.3 Predicting Hazard with CFAST	35
6 Conclusions	42

List of Figures

3.1	CPSC chair fire HRR versus time curves.	9
3.2	CPSC chair fire peak HRR versus time of peak HRR.	10
3.3	Residential scenario schematic	13
3.4	CDF of total residential floor area.	15
3.5	Room area PDF parameters	16
3.6	Room area CDFs	17
3.7	Ceiling height CDF.	18
4.1	Visualization of typical CFAST simulation	24
5.1	Median flashover HRR versus number of samples	29
5.2	PDF of flashover HRR using the MQH correlation	29
5.3	HRR PDFs for cover fabric two	30
5.4	HRR PDFs for cover fabric three	31
5.5	Living room HGL temperature CDFs of barrier fabrics	33
5.6	Living room HGL temperature CDFs of cover fabrics	33
5.7	Convergence of flashover probabilities using MQH based model.	34
5.8	Convergence of critical thermal FED probability in living room.	36
5.9	Bedroom thermal FED CDFs	37
5.10	Bedroom critical thermal FED time CDFs	38
5.11	Living room HGL temperature CDFs	39
5.12	Living room thermal FED versus living room HGL temperature	40
5.13	Bedroom thermal FED versus living room HGL temperature	41
5.14	Average bedroom thermal FED versus average living room HGL temperature	41

List of Tables

3.1 CPSC chair fire HRR peaks	10
3.2 Uncertain building parameters	13
3.3 Constant building parameters	14
3.4 Room area versus home size	15
4.1 Concrete floor properties	25
5.1 Flashover probabilities from inverse MQH	31
5.2 Flashover probabilities from forward MQH	34
5.3 Flashover probabilities by barrier fabric from forward MQH	35
5.4 Probability of lethal conditions in bedroom	37

List of Acronyms

BF	Barrier Fabric
CBUF	Combustion Behaviour of Upholstered Furniture
CDF	Cumulative Distribution Function
CF	Cover Fabric
CFAST	Consolidated Model of Fire and Smoke Transport
CPSC	Consumer Product Safety Commission
FED	Fractional Effective Dose
HGL	Hot Gas Layer
HRR	Heat Release Rate
MQH	McCaffrey, Quintiere, and Harkleroad
NFPA	National Fire Protection Association
NIST	National Institute of Standards and Technology
PDF	Probability Density Function
RUF	Residential Upholstered Furniture

List of Symbols

a	fabric combination label
c_p	specific heat
f_X	probability density function of X
g	gravitational constant
h_w	effective heat transfer coefficient in wall
k	thermal conductivity
l	loss parameters
x	building parameters
A_1	living room area
A_2	bedroom area
A_o	total ventilation area in MQH
F	thermal FED
H	ceiling height
K_x	fire location correction factor
L	random variable for loss parameters
N	number of Monte Carlo samples
T	temperature
T_c	flashover temperature
W_i	width of room i
\dot{Q}	heat release rate
X	random variable for building parameters
\mathcal{D}_{ij}	switch for door between rooms i and j
\mathcal{H}	Heaviside step function
\mathcal{X}	fire location parameter
γ	HRR curve
η_1	living room aspect ratio
θ	controlled parameters
ρ	density
ϕ	indicator function

Abstract

A probabilistic methodology is presented for estimating building fire hazard in the presence of significant scenario uncertainty. This methodology is applied to the specific case of residential upholstered furniture (RUF) fires. The objective of this application is to assess the fire losses associated with different cover fabric and barrier fabric combinations. Several RUF chairs with different fabric combinations are considered. Open furniture calorimeter heat release rate (HRR) data for these chairs was provided by the Consumer Product Safety Commission (CPSC). Residential building statistics are compiled to generate a probabilistic description of typical residential fire scenarios. A correlation and a zone model are used to predict the hazard conditions resulting from these chair fires in an ensemble of residential fire scenarios. Hazard is quantified in terms of the probability of flashover in the room of fire origin and the probability that the thermal fractional effective dose (FED) in an adjacent bedroom is greater than one. It is seen that the predictions of hot gas layer (HGL) temperature using the correlation are significantly higher than those predicted by the zone model. The more accurate zone model indicates that a single RUF chair fire is too small to flashover nearly all rooms considered. However, the zone model results indicate that the choice of barrier fabric significantly affects the HGL temperature. A reduction in the peak HGL temperature of at least 100 ° C was achieved for cases with barrier fabrics other than the worst performer. Even in the absence of flashover, it is possible to produce fatal conditions in an adjacent room for typical RUF chair fires. Barrier fabrics can reduce the probability of lethal conditions occurring in less than 30 min by at least 50 %. Further work is needed to consider the hazard produced by larger furniture and the effects of secondary fuel sources becoming involved in the fire.

Section 1

Introduction

1.1 Objective and Technical Approach

Despite advances in fire protection engineering and flammability standards, residential fire losses remain significant. According to the National Fire Protection Association (NFPA) [1], in the period between years 2009 and 2013, an average of 2470 civilians die each year in home fires. Efforts to reduce the residential fire problem should be focused on the ignition and fuel sources that are most hazardous. Of the fatalities from residential fires, an average of 420 or 17 % resulted from upholstered furniture being the first item ignited [1]. A more detailed analysis of the fire data between years 2006 and 2010 revealed that an additional average of 130 deaths could be attributed to fires in which upholstered furniture was the “primary item contributing to fire spread” [2]. It is clear that residential upholstered furniture (RUF) is a significant part of the national fire problem.

Many technologies have been introduced for reducing the flammability of RUF. Such technologies are effective either by decreasing the probability of ignition or limiting the intensity of an ignited piece of RUF. The goal of reduced flammability is to reduce fire losses—typically thought of in terms of deaths and monetary costs. Introduction of these technologies coincide with industrial, commercial, and environmental costs. It is therefore important to estimate the relative costs and benefits of any proposed flammability reduction technology. One approach for reducing RUF flammability is the addition of a barrier fabric between the upholstery and the padding material. Such barriers act by limiting heat and mass transfer between the padding material and the flame. Barrier fabrics can reduce heat release rate (HRR) of RUF, but it is uncertain to what extent this reduction in HRR affects life safety in typical residential fire scenarios. This report presents some preliminary research on a methodology for estimating the reductions in fire losses corresponding to the use of barrier fabrics in RUF.

The consequences of a fire may be predicted using a fire model. Several classes of fire models are available including simple algebraic correlations, computational two-layer zone models, and computational fluid dynamics (CFD) codes. The choice of model depends on what predictions are necessary, but in all cases some information about the fire scenario is needed. Relevant fire scenario information includes the building geometry (e.g., floor area, ceiling height, ventilation, etc.), construction materials, and the fire burning rate. For many applications such as fire protection engineering or fire scene reconstruction, the scenario parameters are known and can be directly applied as inputs to the model. However, in assessing the overall hazard facing a community, it is

necessary to consider a broad range of scenarios. Two approaches are possible for accounting for the variability in fire scenarios. First, a select number of representative cases could be considered. If these cases are reasonably selected, then the model predictions could be used to estimate the fire hazard in the community. The weakness of this first approach is that it not always clear what cases are representative of realistic fire scenarios in the community. A second approach, and the approach taken in this report, is to estimate probability distributions describing the uncertain parameters in an RUF fire scenario. This method is more challenging because it requires statistics on the various scenario parameters used as inputs to the fire model. A key element of this research then is to gather and analyze the available data on residences in the community. Note that the methodology is general, and can be applied to estimating the effects of other actions intended to reduce fire losses.

Gathering residential building statistics is the first step in estimating fire losses. The second crucial step is a methodology for propagating this variability through the fire model. In almost all realistic applications it is necessary to use a numerical approach for uncertainty propagation. In this report, Monte Carlo (MC) simulation is suggested as robust method for propagating the uncertainty in building parameters through fire models. Because of the large number of simulations required to obtain accurate MC results, an efficient fire model is necessary.

A complete analysis of the potential benefits of a flammability technology should include a consideration of the causes and locations of deaths in residential fires. Gann et al. [3] analyzed the fire statistics between years 1986 and 1990 and found that around 10 times as many deaths outside the room of fire origin were attributed to smoke inhalation as compared to burns. Such data may be used in conjunction with the results presented in this paper to estimate the potential reduction in fatalities associated with the widespread use of an effective barrier fabric.

In this report, the methodology sketched above is described in detail and applied to the case of a single RUF chair with several different cover and barrier fabric combinations. Future work should include the effects of secondary combustible items on the predicted fire losses. Additionally, hazard was quantified exclusively by either the occurrence of flashover or a thermal fractional effective dose (FED), and so a more complete analysis should include the hazard due to toxic gases. The research presented in this report is primarily devoted to developing a methodology for estimating fire losses. The implementation of this methodology is currently in a prototype form, and therefore the emphasis will not be on the predicted results. Future work is necessary to study and improve the data and models, which are essentially inputs into the methodology. It is hoped that improvements to the present prototypical methodology will be suggested and even implemented by a variety of experts interested in reducing the fire problem. In the remainder of this section, a brief survey of the relevant literature is presented, and the remainder of the report is outlined.

1.2 Literature Review

Several similar studies have been reported in the literature. In this section, a brief overview of related work is provided.

Bukowski [4] used a zone model to predict the hazard of various RUF fires in a three room layout. The varied parameters were floor plan geometry, wall materials, heat of combustion of the fuel, the smoke fraction produced, the RUF burning rate, and the presence of an open door. These parameters were typically varied to one or two values other than the nominal values. Hazard was

quantified in terms of gas temperatures, hot gas layer (HGL) height, optical density, and thermal FED. It was found that the hazard criteria are most sensitive to the burning rate of the fuel. The results of this analysis are qualitative due to the limited number of cases considered and the fact that these cases are not rigorously connected to real fire scenarios through well-characterized building data.

The methodology described in the preceding paragraph was implemented in the software HAZARD I [5]. HAZARD I was designed with a focus towards single-family residential structures. The zone model FAST in conjunction with evacuation models were used to predict fire losses. The authors cautioned that the results should only be used for comparisons between products as the models were not developed enough to make precise predictions. The HAZARD I model was applied to a typical ranch home kitchen fire with multiple occupants.

An approach very similar to that of the present report was developed by Clarke et al. [6]. The objective of the referenced research was to use fire and egress models in conjunction with fire data to estimate the change in hazard associated with a change in product. Several applications were studied including the hazard of RUF [7]. The weightings of the specific fire scenario parameters (e.g., time of day, mobility, house size, etc.) were mostly based on data from the national fire statistics. Some of the weightings for RUF were provided by an expert panel. For the furniture application, the modeled fires were assumed to take place in a prototypical ranch home. Fire dynamics and egress were modeled using HAZARD I. The predicted fire deaths compared well with the deaths recorded in the available fire statistics. The research examined the sensitivity of the results to such factors as the locations of the occupants, the potential for occupant rescue, occupant delay in evacuating the house, duration of pre-flaming smoldering, thermal window breakage, and the home size.

The hazard of a single room scenario was explored by Babrauskas [8]. HAZARD I was used to predict the hazard for several cases in which the HRR, toxicity, and ignition time of the RUF fire were varied. Hazard was quantified in terms of gas temperature exceeding 100 °C and the toxicity concentration-time product exceeding 900 g-min/m³. It was concluded that life safety is much more strongly dependent on HRR as compared to toxicity. This is primarily a consequence of the fact that only pre-flashover cases were considered in which the toxicity of gases is relatively low.

Peacock et al. [9] studied flashover using several correlations in addition to the Consolidated Model of Fire and Smoke Transport (CFAST). Flashover is typically defined in terms of the conditions needed to ignite certain target materials within the room of fire origin. Flashover is relevant to hazard in that a post-flashover compartment is certainly untenable and will produce much toxic gas that may be transported to other rooms within the home. Recommended flashover criteria are temperatures exceeding 600 °C and floor heat fluxes greater than 20 kW/m². It was found that correlations such as those of Thomas [10] and McCaffrey et al. [11] are able to predict flashover just as well as CFAST for the scenarios considered. In a continuation of this work, Babrauskas et al. [12] found that there was considerable variability in the occurrence of flashover as a function of HRR in rooms of similar geometry. This variability was attributed to differences in the dynamic behavior of HRR versus time curves. Such behavior is not accounted for in typical correlations. CFAST simulations were used to show that there is a broad range of critical HRRs needed for flashover. Although the critical HRR was found to depend strongly on the time at which flashover occurs, simulations indicate that the results are relatively insensitive to the shape of the HRR curve.

In order to assess the reduction in fire losses associated with a changed mattress flammability

standard, Ohlemiller and Gann [13] used CFAST to predict the spread of smoke throughout a four room structure. This structure was similar to that used by Bukowski [4], but with an additional large compartment to account for the rest of the house. Variations were made to the size of the room of fire origin as well as the door opening fraction. It was found that a reduction in HRR did not eliminate all risk to the occupants, but that it did lead to a much reduced probability that a nearby item would be ignited. From an investigation of fire statistics, it was determined that a significant reduction in HRR would result in a significant reduction in the number of flashovers. Consequently, fire losses would be significantly reduced.

The potential for sublethal incapacitation in fires was studied by Peacock et al. [14] using CFAST. In this work it was noted that a significant limitation of CFAST is an inability to account for the toxicity associated with under-ventilated fires. Three scenarios were simulated: a ranch house, a hotel, and an office. Tenability was accounted for using a thermal FED based on heat and incapacitating asphyxiant gases. Calculation of this FED was based on the models given in ISO 13571 [15]. It was found that time to incapacitation due to heat was much smaller than the time to incapacitation due to asphyxiant gases except for cases of smoldering. Fire deaths due to toxic gas inhalation mostly occur post-flashover.

Several papers have demonstrated methods for propagating uncertainty through fire models. Upadhyay and Ezekoye used the Quadrature Method of Moments (QMOM) to propagate HRR uncertainty through CFAST and an algebraic model for layer height [16]. Layer height cumulative distribution functions (CDFs) were reconstructed using a generalized lambda distribution. The results of the QMOM simulations compared favorably with those obtained by more thorough Monte Carlo simulations. This indicates that efficient methods such as QMOM could be used to adequately propagate uncertainty through fire models.

Monte Carlo simulation of CFAST was used to determine the effects of HRR curve uncertainty on the Available Safe Egress Time (ASET) by Kong et al. [17]. Latin hypercube sampling was used to improve efficiency. Two uncertain parameters, peak HRR and fire growth rate, were considered as random model inputs and modeled as normal or log-normal probability distributions. An extremely large single compartment, representing a commercial building was considered, and the results were presented along with a sensitivity analysis.

From the above discussion, it is clear that both fire hazard analysis and uncertainty propagation are important technical problems. Furthermore, these issues have been studied extensively individually, but relatively little work has been done on the convergence of these two problems. A major contribution of the research presented in this report is a method to use rigorous uncertainty propagation techniques for the analysis of fire hazard in residential scenarios.

1.3 Outline of Report

The objective of this research is to use modeling and simulation to estimate the fire safety benefits of using barrier fabrics in RUF. In the next section, the probabilistic method used to achieve this goal is described. Section 3 presents the data needed to apply the methodology to the problem of RUF fires. The two fire models used to predict fire hazard from the uncertain inputs are discussed in Sec. 4. Results are presented in Sec. 5, and summarized in Sec. 6. Note that confidence in the estimated fire losses depends on the quality of both the models and the data, and future work will be directed towards increasing this confidence.

Section 2

Predicting Fire Losses

2.1 Models for Fire Losses

To investigate the potential benefits of using barrier fabrics in residential upholstered furniture (RUF), it is necessary to have a method for using available data to predict these benefits. In fire safety, the benefit of an action is typically measured by the resultant reduction in fatalities or property loss. Thus, the most beneficial action is the one with the smallest estimated *fire losses*. In this section, a probabilistic approach is presented for using fire models to estimate fire losses.

It is helpful to begin by developing a mathematical formalism for describing the loss due to a fire and its relationship to the relevant details of the home in which that fire takes place. That relationship is essentially a fire model. For example, there are several algebraic correlations used to predict the temperature in a compartment as a function of the heat release rate (HRR) of a fire. In addition to the HRR, such correlations will require some information on the size and shape of the compartment. So in this case, the temperature is the loss metric (as a surrogate since higher temperatures are more likely to result in deaths and structural damage), the correlation is the fire model, and the HRR and compartment geometry are the scenario parameters. For this report, the situation is complicated because the scenario parameters and, consequently, the loss metric are uncertain. In order to avoid ambiguity, the preceding discussion is now described mathematically.

The fire losses may be quantified as l , representing monetary costs, deaths, resources, or any other appropriate measure. The loss metric l can be applied to a building, community, state, nation, or any other system susceptible to fire. To evaluate the effectiveness of an action (e.g., the selection of a barrier fabric), the action must be parameterized through a set of *controlled parameters*, θ . It is important to emphasize that the controlled parameters are chosen by an engineer or decision maker. For example, in the case of barrier fabrics, θ could denote different types of barriers, and the RUF manufacturer has complete freedom to select whatever barrier fabric that most satisfies their design and safety requirements.

Fire scenarios can vary considerably, and so it is necessary to approach the problem probabilistically. In the field of probability and statistics, it is common to distinguish the value actually taken by a random variable and the random variable itself. This is accomplished notationally by using an upper case letter for the random variable, and the lower case equivalent for the value of a particular instantiation of that variable. The random variable for loss is thus denoted as L . The appropriate representation of a random variable is a probability distribution. The remainder of this

section will involve describing how to use fire models in conjunction with relevant data to estimate the probability distribution for fire losses given a choice of the controlled parameters. This probability distribution will be denoted as $f_L(l|\theta)$ if l is a continuous variable, or $\Pr(L = l|\theta)$ if l is a discretely distributed variable.

Determination of a probability distribution for L in terms of the controlled parameters, requires a model relating the loss metric, l , to θ . Such a loss model will typically consist of a fire model component that relates the physical parameters describing the scenario, x , to the resultant environmental conditions in a structure as a consequence of a fire. Fire models can range from simple empirical correlations to sophisticated computational fluid dynamics (CFD) software.

A complete loss model requires additional considerations beyond the purely physical nature of a fire model. Loss models may be extremely complicated, especially if the loss metric involves human life. Such loss models require knowledge of physiology, human mobility, as well as fire detection and suppression technologies. In the present work, evacuation, detection, and suppression are not considered.

Conceptually, a loss model can be thought of as a map of the scenario parameters to the loss metric:

$$l = g(x) \quad (2.1)$$

In words, the loss model, g , takes the input scenario parameters, x , and predicts the loss metric, l . Equation (2.1) gives a single deterministic result for a single specified scenario. Therefore, Eq. (2.1) requires that the scenario described by x is known. It is further assumed that the scenario parameters are dependent on the controlled parameters, θ , in some way. That is, in order for the effect of the controlled parameter to be evaluated, it is necessary that θ have some effect on the scenario as it is described by the loss model. The simplest relationship would just be that one of the scenario parameters is the controlled parameter. For example, the scenario parameters could be the set $x = \{a, b, \theta\}$.

In general, the scenario is not precisely known and must be characterized as a set of random variables, X . The uncertainty of the scenario must be characterized from relevant statistics. The procedure of determining and applying these statistics is demonstrated in Sec. 3, but first it is appropriate to discuss how such information may be used to estimate fire loss probabilities.

2.2 Estimating Fire Loss Probabilities

The problem is to determine the uncertainty in fire losses from the uncertainty in the scenario. The approach taken to solve this problem is to use Monte Carlo simulation. In the context of uncertainty propagation, Monte Carlo simulation is the procedure of running a model many times for many different scenarios and then using the results to characterize the uncertainty in the outputs. The simulated scenarios are sampled from probability distributions describing the uncertainty in these parameters. For the example of a compartment temperature correlation, one would simply randomly select many values of HRR and compartment sizes to get a large number of predicted compartment temperatures. If the sampled values of HRR and the compartment sizes are representative of the uncertainty in these parameters, then the set of predicted values will be representative of the compartment temperature uncertainties. The process is straightforward, but a more mathematical description is given in the following for the sake of precision.

It is assumed that probability distributions for the scenario parameters are known. These parameters may be continuous or discrete and the uncertainty will be characterized by a mixed joint density function conditional on the controlled parameters, $f_X(x|\theta)$. In the following, it will be assumed that the loss metric is discretely distributed, but the continuous case is analogous. The relationship between the probability distribution for L and the probability distribution for X is

$$\Pr(L = l | \theta) = \int dx f_X(x|\theta) \phi[l = g(x)] \quad (2.2)$$

where $\phi[l = g(x)]$ is the indicator function that evaluates to one if $g(x) = l$ and is otherwise zero.

The integral in Eq. (2.2) is usually impossible to evaluate analytically. Fortunately, the problem is readily amenable to Monte Carlo simulation where the integral is approximated as

$$\Pr(L = l | \theta) \approx \frac{1}{N} \sum_{i=1}^N \phi[l = g(x_i)] \quad (2.3)$$

where the x_i are N samples from X . In practice, this requires a large number of samples, especially as the dimensionality of X increases. It is therefore necessary to have relatively efficient fire and loss models. An additional use of the Monte Carlo samples is to compute the expected value of L . This approximation is made from the samples using

$$\langle L(\theta) \rangle = \frac{1}{N} \sum_{i=1}^N g(x_i) \quad (2.4)$$

It will typically take fewer samples to accurately estimate $\langle L \rangle$ than it will to approximate $\Pr(L = l)$.

An more efficient alternative to Monte Carlo simulations is the quadrature method of moments (QMOM), which has been used to propagate uncertainty through fire models [16]. Although this procedure will not be used in the following, it is a potential tool for use in future extensions of this work.

Generally, there will be multiple scenario parameters, and $f_X(x|\theta)$ will be multivariate. Sampling from a multivariate function is not straightforward. For many cases, the random variables composing X will be independent. In such cases, the marginal distributions may be sampled separately. For cases in which the statistical model may be represented by a directed graph, it is possible to decompose the joint probability distribution into a product of conditional distributions. The set of model parameters is first partitioned into M subsets denoted x_i for $i = 1, \dots, M$. The joint distribution function is then written as

$$f_X(x) = \prod_i^M f_{X_i}(x_i|x_i^*) \quad (2.5)$$

where x_i^* represent all variables upon which the set x_i depends. This representation makes it possible to do ancestral sampling of the joint distribution. For the simple case of one variable, X_2 having a known probability distribution conditional on the values of another variable, X_1 , the joint distribution is sampled by taking random samples, $x_{1,i}$, from f_{X_1} and subsequently obtaining the samples $x_{2,i}$ by sampling from $f_{X_2}(x_2|x_{1,i})$.

The next section will discuss characterizing f_X for residential structures in the United States. This will involve collecting data for residential building geometries. Additionally, data is presented relating the controlled parameter, θ , which in this case is a label for a particular cover and barrier fabric combination, to one of the uncertain model parameters, which in this case is a HRR curve.

Section 3

Data

3.1 Overview

In order to analyze the consequences of a change in some controllable parameter θ , it is necessary to determine both the relationship of θ to the fire model and the probability distribution of the scenario parameters, X . In this section, the relevant data is compiled. The controllable parameter is the cover and barrier fabric combination used in an residential upholstered furniture (RUF) chair. The relationship between a particular fabric combination and the fire model is provided by experimental heat release rate (HRR) data for several chairs. A generic residential fire scenario is presented, and relevant building statistics for that scenario are collected, and summarized as probability distributions.

3.2 Chair Fire Data

The chair fire data were provided by the Consumer Products Safety Commission (CPSC). Experiments were performed in an open furniture calorimeter, and the relevant data is the HRR as a function of time. The HRR associated with these tests will tend to be different than that experienced by an identical chair burning in a compartment due to decreased ventilation and heat feedback from the walls. A decrease in ventilation can reduce the oxygen supply enough to reduce the gas phase combustion, but the available oxygen is not typically reduced significantly prior to flashover. Heat feedback from compartment walls and the hot gas layer (HGL) can cause the HRR to increase [18]. The CPSC tests were performed on chairs with the same geometry, foam, and construction. Three variables distinguished the tests: the cover fabric, the barrier fabric, and whether the chair had been repeatedly stressed. Note that the terminology “cover fabric” is used here to denote the outer layer of upholstery fabric. In cigarette smoldering tests, “cover fabric” typically refers to a small piece of fabric placed on top of the smoldering cigarette. For the purposes of this analysis, only the fabric combination was considered since the degree of stress a piece of furniture has experienced cannot be controlled in residential settings. Two cover fabrics were used. Both of these cover fabrics were tested four to seven times with one of six different barrier fabrics.

A total of 68 tests were analyzed. The HRR curves for all of these tests are plotted in Fig. 3.1 where the results have been separated into (a) cover fabric 2 and (b) cover fabric (3). In many of

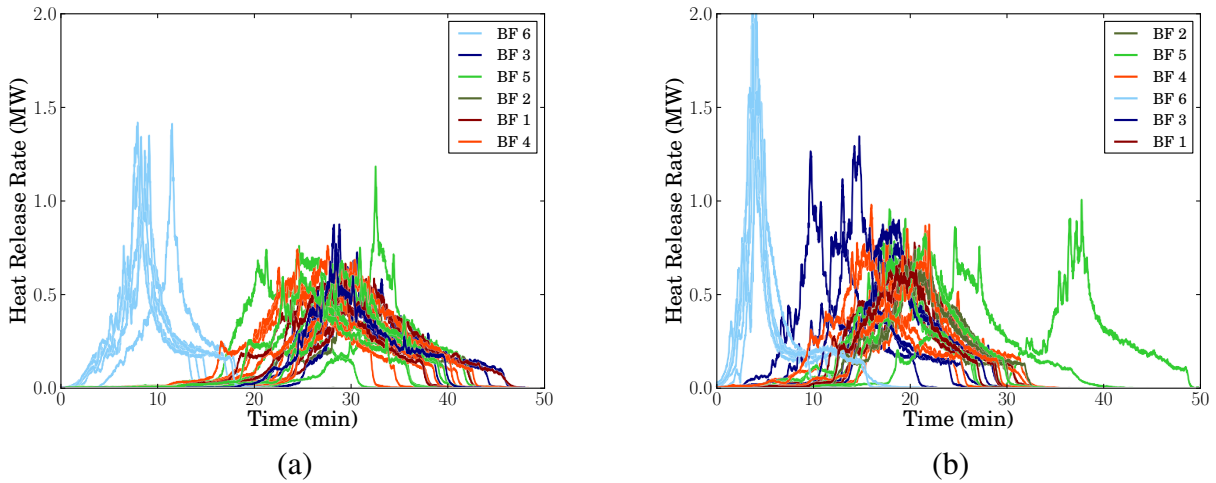


Figure 3.1: CPSC chair fire HRR versus time curves for (a) cover fabric 2 and (b) cover fabric 3. “BF” denotes “Barrier Fabric”.

the figures in this report, “CF” and “BF” will be used as shorthand for “Cover Fabric” and “Barrier Fabric”, respectively. It is clear from Fig. 3.1 that the choice of cover and barrier fabric can have a significant influence on the time and value of the HRR peak. For cover fabric 2, the difference between barrier fabric 6 and the other barrier fabrics is significant.

To see these trends more clearly, a summary of the data in terms of the HRR peak is presented as a scatter plot in Fig. 3.2. The error bars Fig. 3.2 represent one standard deviation of the experimental data. The mean and standard deviation of the peak HRR data are tabulated in Table 3.1. Clearly, chairs using barrier fabric 6 have the highest peak HRR by a significant amount for both cover fabrics. It is also apparent that use of cover fabric 3 typically results in more intense fires. At the other end of the spectrum barrier fabric 2 seems to provide a significant amount of flammability reduction when coupled with either cover fabric. In general, it is seen that as the peak HRR decreases, the time until that peak is reached increases. This is explained by the fact that all chairs have about the same total heat release (integrated HRR), and so extending the fire over greater time results in a lower peak HRR.

The data presented above will be used as input into the loss models described in Sec. 4. These models predict the effects of a given fire in a compartment. It will be assumed that the burning rate of the chairs will be the same in the compartments as it was in the open calorimeter. This is not strictly valid because of heat feedback and potential ventilation effects that are absent in the furniture calorimeter. Some research has suggested that for fires with peak HRRs greater than around 2 MW, the HRR is relatively insensitive to enclosure effects [19]. A more recent and comprehensive research project, The Combustion Behaviour of Upholstered Furniture (CBUF) programme [18] compared peak HRRs measured in a furniture calorimeter to those measured in a room calorimeter. For peak HRRs less than 100 kW, there is little disparity between the room and open calorimeter results. Most of the data correspond to furniture that produced peak HRRs in the range of 400 kW to 1 MW in the furniture calorimeter. For most of this data, the furniture calorimeter tends to underpredict the corresponding room value. For some cases, the underprediction can be up to nearly

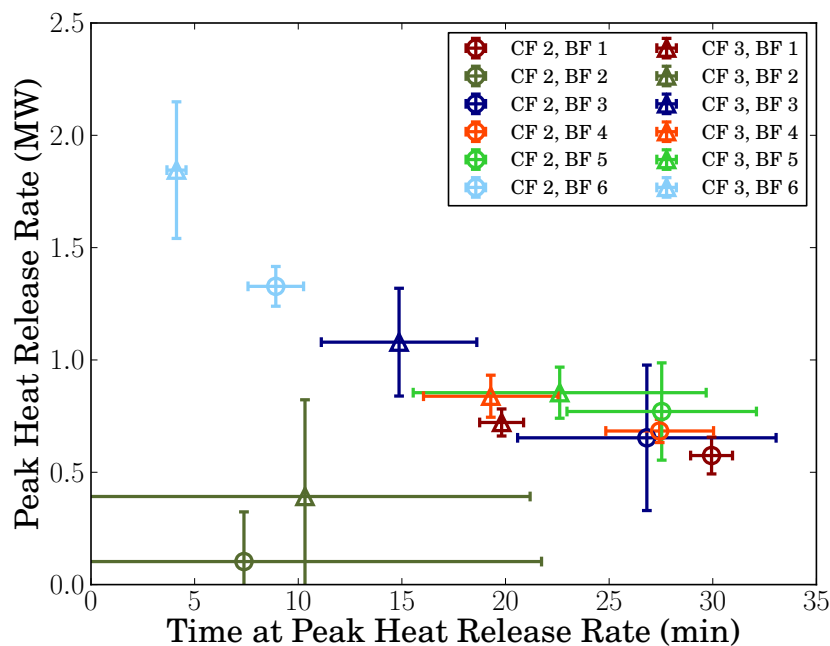


Figure 3.2: Average CPSC chair fire peak HRR versus average time to peak HRR.

Table 3.1: CPSC chair fire peak HRR mean and standard deviation.

Cover Fabric	Barrier Fabric	Replicates	Time of Peak HRR (min)	Peak HRR (MW)
2	1	4	29.9 ± 1.0	0.57 ± 0.08
2	2	5	7.4 ± 14.4	0.10 ± 0.22
2	3	6	26.8 ± 6.2	0.65 ± 0.32
2	4	7	27.4 ± 2.6	0.68 ± 0.05
2	5	6	27.5 ± 4.6	0.77 ± 0.22
2	6	6	8.9 ± 1.3	1.33 ± 0.09
3	1	4	19.8 ± 1.1	0.72 ± 0.06
3	2	6	10.3 ± 10.9	0.39 ± 0.43
3	3	5	14.9 ± 3.8	1.08 ± 0.24
3	4	6	19.3 ± 3.2	0.84 ± 0.09
3	5	7	22.6 ± 7.1	0.85 ± 0.11
3	6	6	4.1 ± 0.5	1.85 ± 0.30

600 kW. Since many of the chair fires considered in this report have peak HRRs in this range (see Table 3.1), it is necessary to note that the fire hazard might be underpredicted.

As an aid to relating the RUF HRR data to the loss models, it is helpful to make reference to some of the theory of Sec. 2. The controlled parameter for all cases is the fabric combination, and so it is appropriate to define θ as the tuple of $a \equiv (\text{cf}, \text{bf})$ where cf and bf are the cover and barrier fabric labels, respectively. This ordered pair influences the fire model through the HRR, \dot{Q} , which will be treated as an uncertain scenario parameter, \dot{Q}^* —here the superscripted asterisk denotes that the variable is a random variable. Three approaches are taken for the two loss models. The first two approaches are for sampling just the peak HRR, while the third approach is for sampling the entire HRR versus time curve. The first and second sampling approaches are distinguished by the underlying distribution. In the first approach, the sampled values are taken to be one of the experimentally measured peak HRRs for a particular fabric combination. The second approach is based on sampling from a continuous probability density function (PDF) that was fit to the experimental data. The first and third approaches utilize discrete probability distributions, while the second approach utilizes a continuous probability distribution. The choice of approach for modeling the HRR uncertainty will depend on the model and the method used. In the analysis of this report, all three approaches will be used. These approaches are described formally in the following paragraphs.

In some cases, only the peak HRR, \dot{Q}_p is necessary. So the first approach is to just sample from the available experimental peak HRR values for a given fabric combination. Assuming a uniform distribution among the measured values, the appropriate probability distribution is

$$\Pr(\dot{Q}_p^* = \dot{Q}_{p,j}|a) = \frac{1}{N_a}, \quad j = 1, \dots, N_a \quad (3.1)$$

where $\dot{Q}_{p,j}$ is one of the measured peak HRRs for fabric combination a , and N_a is the number of replicate experiments for fabric combination a (see the third column in Table 3.1).

A second approach is possible when only the peak HRR is needed. In this approach, the statistics listed in Table 3.1 are used to define a probability density function (PDF) for the peak HRR. In many physical processes, a normal distribution is a reasonable model of stochastic behavior. However, the requirement that $\dot{Q} > 0$ necessitates the use of a truncated normal distribution. For distributions truncated at zero, this PDF assumes the form

$$f_{\dot{Q}_p^*}(\dot{Q}_p|a) = \frac{\exp\left[-(\dot{Q}_p - \mu_a)^2 / 2\sigma_a^2\right]}{\sigma_a\sqrt{2\pi} \left\{1 - \frac{1}{2} \left[1 + \operatorname{erf}\left(-\mu_a / \sigma_a\sqrt{2}\right)\right]\right\}} \quad (3.2)$$

where μ_a and σ_a are the mean and standard deviation for the peak HRR of combination a as listed in the last column of Table 3.1.

A third approach is needed for cases in which the entire HRR versus time curve is needed. In such scenarios, it is appropriate to sample the experimental curves directly. Since the full HRR curve must be represented by a large number of points, it is not straightforward to develop statistical models for each point in the curve. Therefore, a sample will be an entire experimental HRR curve represented as a set of time-HRR pairs: $\gamma \equiv \{(t, \dot{Q})\}_i$. Each experiment corresponds to a set of time-HRR pairs, and the probability of sampling a single γ will be uniform across the

available HRR curves for a given fabric combination, a . That is, if γ_j denotes a time-HRR curve corresponding to fabric combination a , then

$$\Pr(\Gamma = \gamma_j|a) = \frac{1}{N_a}, \quad j = 1, \dots, N_a \quad (3.3)$$

The choice of using Eq. (3.1), Eq. (3.2), or Eq. (3.3) will depend primarily on what information is required by the model. As will be seen in Sec. 4, the MQH correlation requires that only a single value of \dot{Q} be given. For all of the MQH calculations then, either Eq. (3.1) or Eq. (3.2) will be used. Conversely, for the CFAST model, a time dependent HRR curve is required, and so Eq. (3.3) must be used.

3.3 Building Statistics

The consequences of a RUF fire depend on the scenario. The scenario is defined by the building, its contents, and the people present at the time of the fire. Residential buildings are exceptionally varied in construction so not all potential scenarios can be analyzed. However, it is possible to design a representative set of residential structures by reference to the appropriate building statistics. A generic three room building section is presented. This building section is characterized by several variables. Some of these parameters are assumed to be known. Other building parameters are uncertain. These uncertain variables are characterized by the probability distributions presented in this section.

Previous researchers have used three room models to analyze the effects of furniture fires (e.g., in [4]). Such models allow for the examination of fire hazard in both the room of origin as well as in connected rooms. The generic model used in the present research is sketched in Fig. 3.3. In this set of scenarios, it is assumed that the fire occurs in the living room, which has a floor area of A_1 . The geometry of this room influences heat losses, and so the aspect ratio of the room, $\eta_1 \equiv L_1/W_1$, must be considered. Since the location of the fire with respect to the walls can have a significant effect on the development of the hot gas layer (HGL), it is necessary to introduce a fire location parameter, \mathcal{X} , that specifies whether the fire is in the center of the room, against a wall, or in a corner. Hot gases from the fire can spread through the doors, \mathcal{D}_{12} , \mathcal{D}_{13} , and \mathcal{D}_{23} , which may or may not be open. Hot gases can spread down the hall, which has a variable width of W_3 , but the length of the hallway is determined by A_1 , η_1 , and the area of the bedroom, A_2 . The ceiling height, H , is assumed to be the same throughout the home. Note that the generic home model of Fig. 3.3 will have a limited supply of oxygen due to the assumption that all ventilation to the remainder of the house is closed. No data was found on whether this assumption is typical of U.S. homes, but future work should examine the sensitivity of the hazard assessments to the availability of additional air from non-participating compartments.

A list of all of the variable building parameters is provided in Table 3.2. For each of these parameters, a probability distribution must be determined. Before discussing this, however, a few constant parameters will be introduced.

Several of the building parameters required by the models are assumed to be constant. Based on minimum requirements from the International Residential Code (IRC) [20], the door heights

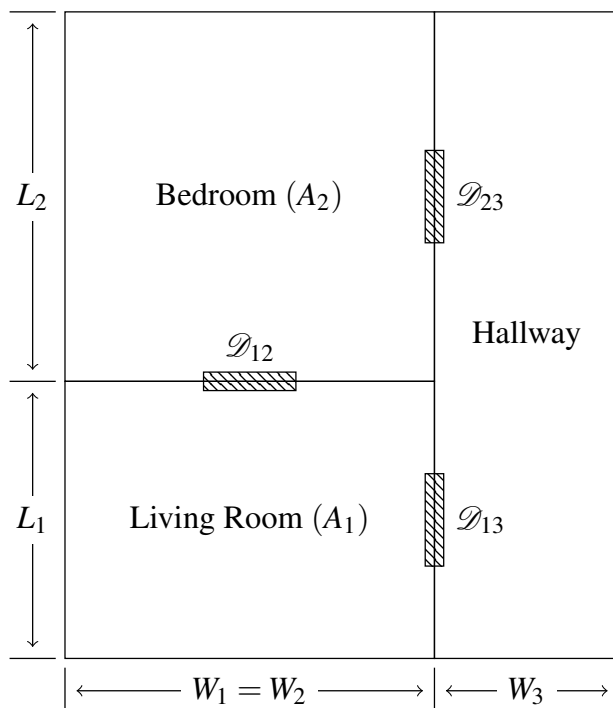


Figure 3.3: Schematic of three-room layout for residential fire scenarios.

Table 3.2: Random variable building parameters considered in analysis.

Parameter	Notation (units)
Living Room Area	A_1 (m ²)
Bedroom Area	A_2 (m ²)
Living Room Aspect Ratio	η_1 (-)
Ceiling Height	H (m)
Door Openings	\mathcal{D}_{ij} (-)
Hall Width	W_3 (m)
Fire Location	\mathcal{X} (-)

Table 3.3: Constant building parameters used in models.

Parameter	Notation (units)	Value
Door Height	H_d (m)	1.98
Door Width	W_d (m)	0.81
Wall Thickness	L_w (m)	0.0127
Wall Thermal Conductivity	k_w (W/m·K)	0.28
Wall Density	ρ_w (kg/m ³)	810
Wall Specific Heat Capacity	c_w (J/kg·K)	1000
Ambient Temperature	T_∞ (K)	295.15

are held constant at 78 in (1.98 m), and the door widths are always 32 in (0.81 m). The walls are assumed to be made of standard 0.5 in (0.0127 m) gypsum wallboard. Thermophysical properties of the gypsum were taken from reference [21]. An ambient temperature of 22 °C (295.15 K) is in all simulations. A summary of the constant parameters is provided in Table 3.3.

In the remainder of this section, probability distributions are specified for each of the uncertain building parameters. These distributions are based on available data as much as possible. In cases where the data were unavailable, the minimal assumption about the variable was assumed—in most cases, the minimal assumption is that of a uniform probability for all possible values. Improvements to the analysis can be made by the application of better data to the stochastic representation of the scenario.

As a preliminary to developing realistic probability distributions for the living room and bedroom areas (A_1 and A_2 , respectively), data on the total square footage of residential units was sought. Such data were obtained from the United States Census Bureau’s 2013 American Housing Survey (AHS) [22]. The results of this survey include information on the number of residential units in a given range of floor area. The data from the AHS does not include explicit lower and upper bounds. That is, the lower bin is given as including all homes with square footage less than 500 ft², and the upper bin is given as including all homes with square footage greater than 4000 ft². Therefore, it was necessary to make assumptions on the lower and upper bounds of the data. An assumed minimum of 400 ft² (37.2 m²) and a maximum of 6000 ft² (557.4 m²) were selected. The results should not be too sensitive to this choice of bounds since they represent a small portion of the total probability mass. This data is represented as a cumulative distribution function (CDF) in Fig. 3.4.

The data on total home area was used in conjunction with results from the National Association of Home Builders (NAHB) [23] to arrive at estimates on the distributions of living room and bedroom floor areas. The NAHB report [23] surveyed builders of single-family homes on the distribution of total home area between the various rooms in the house. In particular, the average area of the master bedroom and the living room were reported for homes of “small”, “average”, and “large” sizes. This data is provided in Table 3.4.

Lines were fit to this data to give relationships for the average room floor areas, A_1 and A_2 , as functions of the total home area, A_T . These lines could be used to obtain samples of A_1 and A_2 given a sampled value of A_T in accordance with the ancestral sampling procedure described

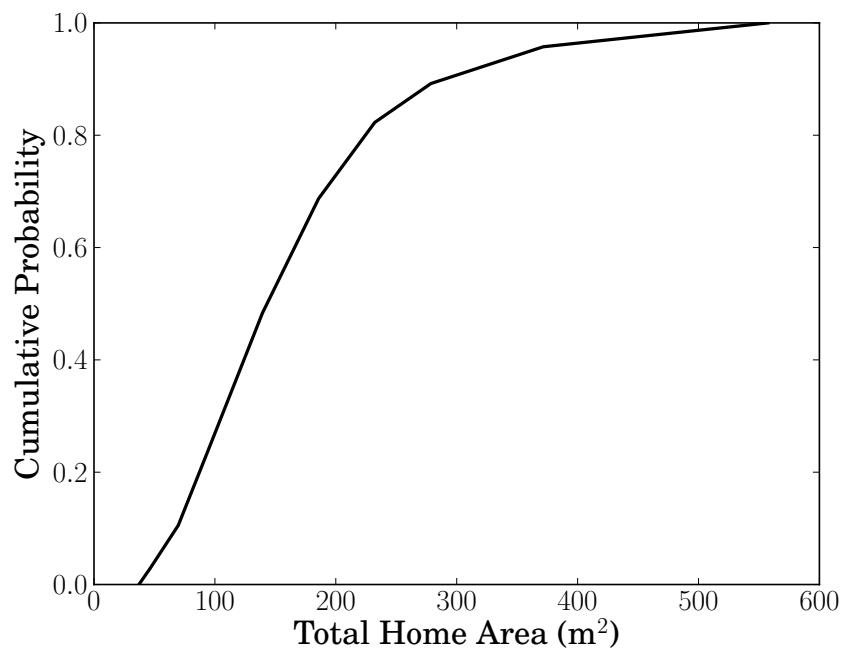


Figure 3.4: Cumulative distribution function (CDF) of total residential floor area.

Table 3.4: Average room floor area from NAHB data [23]

Home Size	Total Home (m ²)	Living Room (m ²)	Bedroom (m ²)
Small	151	17.9	21.4
Average	240	20.7	28.7
Large	351	26.2	38.2

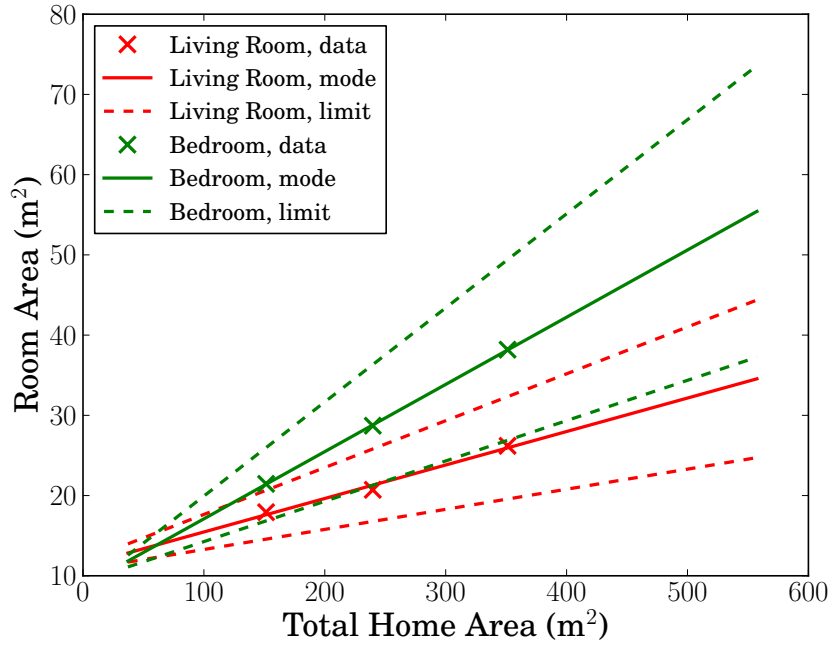


Figure 3.5: Room area triangular PDF parameters as a function of total home area.

at the end of Sec. 2. However, there is likely to be some variability in the relationship between the room floor areas and the total home floor area. Such variability was allowed for by assuming triangular probability distributions about the average values for the living room and bedroom areas. Triangular distributions are three parameter PDFs requiring lower and upper bounds in addition to the peak value. Symmetric distributions are assumed so that the peak value, $A_{i,p}$ is just the average value predicted from the correlation between the room and total areas. The lower and upper bounds were determined as $A_{i,p} \pm \delta (A_{i,p} - A_{\min})$ for $i = 1, 2$ where δ was chosen to be 0.4 and $A_{\min} = 10 \text{ m}^2$. These parameter values are somewhat arbitrary, but they reasonably represent the large uncertainty in room area variation. A plot of the three triangular distribution parameters along with the NAHB data is provided in Fig. 3.5.

Samples for the living room and bedroom areas were obtained from ancestral sampling as follows. A sample of the total home area, $A_{T,i}$ was obtained from the CDF plotted in Fig. 3.4. Corresponding samples for $A_{1,i}$ and $A_{2,i}$ were taken from the triangular distributions with parameters corresponding to the lines plotted in Fig. 3.5. The resultant CDFs for the room areas are shown in Fig. 3.6. It is seen that the median room areas are around 20 m^2 .

The next uncertain parameter to be considered is the living room aspect ratio, η_1 . No data was found on this parameter, and so a uniform distribution was assumed between the bounds of 0.5 and 1. Note that it is not necessary to extend this distribution above 1 since this would just replicate a room geometry below 1. For example, two rooms of the same floor area and with aspect ratios of $3/4$ and $4/3$ are equivalent.

Ceiling height data was obtained from the U.S. Energy Information Administration’s Residential Energy Consumption Survey (RECS) [24]. In response to the question of whether they had

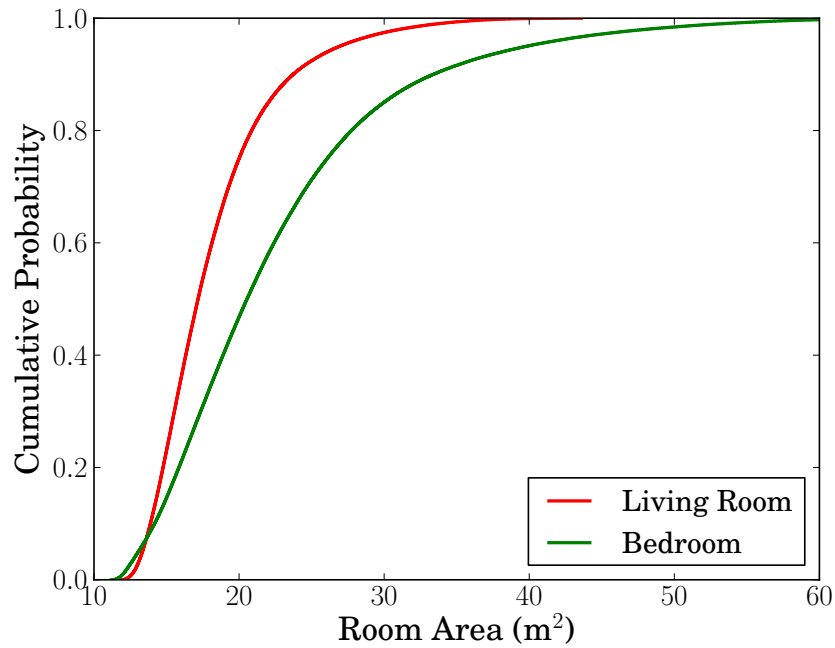


Figure 3.6: Cumulative distribution functions (CDFs) for room floor areas.

“unusually high ceilings” (defined as greater than 8 ft (2.44 m), 27 % of respondents replied “yes”. A piecewise linear CDF was assumed since no other information was found. A lower bound was chosen of 7 ft (2.13 m) based on the minimum height in the IRC [20]. The upper bound on ceiling height was estimated to be 10 ft (3.05 m). The resultant CDF for ceiling height is plotted in Fig. 3.7.

It is significantly more difficult to estimate the likelihood that any of the doors shown in Fig. 3.3 will be open. The state of the doors will be represented by the 3-tuple $\mathcal{D} \equiv (\mathcal{D}_{12}, \mathcal{D}_{13}, \mathcal{D}_{23})$, where the elements of \mathcal{D} assume values of 1 if that door is open and zero if that door is closed. For scenarios in which both living room doors are closed, it is impossible for occupants in other rooms to be at risk (at least under the assumptions of the model). Furthermore, flashover is not really well-defined for under-ventilated compartments. In order to avoid the case with no ventilation, it is assumed that at least one of the living room doors is opened. This results in a total of six possible cases for the door state tuple: (1,0,0), (0,1,0), (1,1,0), (1,0,1), (1,1,1), and (0,1,1). It is assumed that the probabilities of these six states are the same and therefore equal 1/6.

The width of the hall, W_3 , is uncertain. A lower bound of 3 ft (0.91 m) is chosen based on the requirement of the IRC [20]. The upper bound was assumed to be equal to 6 ft (1.83 m). A uniform PDF was assumed between these two values. It is likely that there is a strong correlation between W_3 and the total area of the home, A_T . However, this correlation is unknown at present, and so W_3 is allowed to be independent of A_T .

The final uncertain parameter that must be characterized is the fire location parameter, \mathcal{X} . The necessity of including this parameter is due to the fact that the HGL temperatures are significantly increased if the fire is next to a wall or in a corner. Therefore, \mathcal{X} is allowed to be discretely

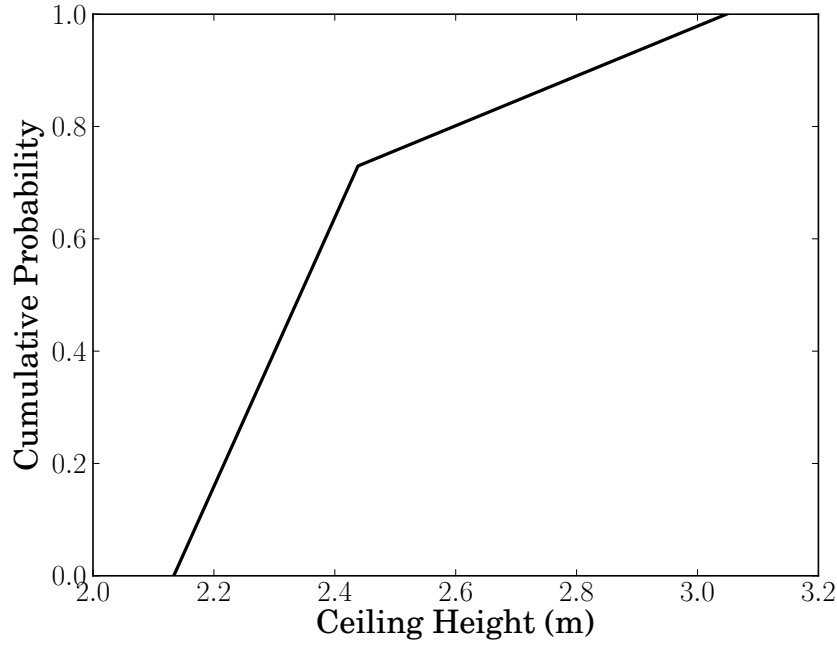


Figure 3.7: Cumulative distribution function (CDF) for ceiling height.

distributed between locations in the center of the room, against a wall, or in a corner. No data is available on how people actually distribute furniture in their homes, and so the minimal assumption of uniform probability is required once again. In particular, it is reasonable that the furniture be at any location in the room with equal probability. It is more likely that a piece of RUF will be in a corner or against a wall in a smaller room as compared to a larger room. Thus, the probability of the furniture being in one of the three possible locations is assumed to be proportional to the relative area of that location for the given room. It is apparent that these probabilities are

$$\Pr(\mathcal{X} = \text{Corner}) = \frac{4L_f^2}{A_1} \quad (3.4)$$

$$\Pr(\mathcal{X} = \text{Wall}) = \frac{2L_f(W_1 + L_1) - 4L_f^2}{A_1} \quad (3.5)$$

$$\Pr(\mathcal{X} = \text{Center}) = 1 - \Pr(\mathcal{X} = \text{Corner}) - \Pr(\mathcal{X} = \text{Wall}) \quad (3.6)$$

where L_f is the characteristic dimension of the furniture. Note that this model assumes that the furniture is approximately square, and that furniture can be located in front of open doors. The first assumption is acceptable for the purposes of this research as square RUF chairs are the fuel source. The second assumption will have little effect for most rooms as the door width is much less than the perimeter of the living room. Because the probabilities in Eqs. (3.4)-(3.6) are conditional upon the area and aspect ratio of the living room, it is necessary to use the ancestral sampling procedure described at the end of Sec. 2 in which samples for A_1 and η_1 are generated and then used to generate a sampled value of \mathcal{X} .

All of the uncertain parameters listed in Table 3.2 have been characterized in terms of probability distributions. In general, samples are produced through random number generation and the

inverse CDFs of the building parameters. In some cases, the SciPy “stats” module [25] is used to draw samples from discretely distributed random variables. The samples must be drawn in a specific order due to the dependencies discussed above. Specifically, a total room area sample must precede the room area samples, and the living room area and aspect ratio samples must precede the fire location sample.

The probability distributions presented in this section were used to estimate fire losses. This is achieved by Monte Carlo simulations in which samples from these probability distributions are used as inputs to one of two fire models. In the next section, these fire models are discussed.

Section 4

Model Descriptions

4.1 Overview and Selection of Loss Metrics

The selection of an appropriate loss model is a coupled process. First, the appropriate loss metric, l , must be selected, and then a model must be found that predicts l . That model will depend on some set of environmental parameters, and a fire model must be chosen that predicts these quantities. The controlled parameters, θ , must have some influence on the fire model or its input parameters so that the effects of varying these parameters can be studied.

In this section, two loss models are described. The first is based on an empirical correlation for the hot gas layer temperature (HGL) in the room of fire origin—in this case, the living room. The second model is based on a zone model used to predict HGL temperature and height in all three rooms of the test home described in the previous chapter. In both cases, the loss metric is assumed to be the occurrence of fatal conditions in the house during the course of the fire. This definition for l does not equate to the number of fatalities since no assumptions have been made with regard to the presence of people in the home. Future work should incorporate a statistical description of the presence of people throughout the home. Such a description would extend the results of the present work beyond a rough measure of the potential for fatalities to the actual expected number of fatalities.

Predicting fatalities depends on many different factors such as the number and age of building occupants as well as the presence of smoke detectors or sprinklers. While consideration of evacuation, detection, and suppression is a possible avenue for future work, such factors are beyond the scope of the present research. In this report, two criteria are used to evaluate tenability: transition to flashover and thermal fractional effective dose (FED).

After a compartment has transitioned to flashover, most combustibles in the room will be burning, and the fire will be under-ventilated. In all cases, the compartment will be uninhabitable, and hot, toxic gases will be transported throughout the residence. Therefore, occupants in connecting rooms are at considerable risk in a post-flashover scenario. It has been suggested that compartment fires transition to flashover once the HGL temperature exceeds 500 °C to 600 °C [10]. For cases in which the ambient temperature is 22 °C, this results in a range of flashover temperature rises of ΔT between 478 °C and 578 °C. In the analysis of Sec. 5, it will be assumed that a temperature rise of 500 °C results in flashover. Using a temperature from the lower end of the flashover range is a conservative estimate as it will tend to over-predict the frequency of flashover. Future work should

consider the sensitivity of the results to the choice of flashover temperature.

The second loss model is based on the concept of a thermal FED. The thermal FED is the ratio of the dose received to a critical dose usually associated with lethality or incapacitation [26]. The dose is typically associated with a toxic gas (e.g., carbon monoxide or hydrogen cyanide) or heat exposure. In this case, only the hazard associated with heat is considered, since the production of toxic gases is relatively small for well-ventilated, pre-flashover fires. There is some literature to indicate that, indeed, heat exposure represents a significantly greater threat to life safety as compared to toxic gases in residential fires [14]. It is recommended [15] that the thermal FED be computed as

$$F(t) = \int_0^t \left(\frac{(q''(t'))^{1.33}}{r} + \frac{(T(t'))^{3.4}}{5 \times 10^7} \right) dt' \quad (4.1)$$

where q'' is the radiant heat flux in kW/m², r is the radiant exposure dose, and T is the temperature in °C. All times are in minutes. Equation 4.1 accounts for both exposure of skin to radiant and convective heat. The choice of r depends on what threshold is appropriate. For the analysis of this report, a value of $r = 16.7$ will be used as representative of a dose resulting in 50 % fatalities for the average population. Note that incapacitations could occur at thresholds much lower than this, especially for vulnerable populations. The choice of r was made in order to consider the most serious risks to the occupants and is therefore not conservative. Future analysis should take into account a range of critical radiation threshold values.

Fatal conditions are predicted by both the transition to flashover of the room of fire origin and the thermal FED in the living room. The application of these models in conjunction with the data presented in Sec. 3 will be used in Sec. 5 to predict the probability of lethal conditions in a fire associated with a given fabric combination.

4.2 Empirical Correlation

Several correlations have been developed for estimating temperatures in compartment fires [27]. Such correlations are typically based on an energy balance where unknown parameters are lumped together and then calibrated to experimental data. A widely used correlation for hot gas layer (HGL) temperature in naturally ventilated compartments was developed by McCaffrey, Quintiere, and Harkleroad [11]. This so-called MQH correlation was fit to data from over 100 experimental sets, and has been validated against several sets of additional data [28]. The basic form of the MQH correlation is

$$\frac{\Delta T}{T_\infty} = 1.63K_x \left(\frac{\dot{Q}}{\rho_\infty c_{p,\infty} A_o \sqrt{gH_o T_\infty}} \right)^{2/3} \left(\frac{h_w A_w}{\rho_\infty c_{p,\infty} A_o \sqrt{gH_o}} \right)^{-1/3} \quad (4.2)$$

where $\Delta T \equiv T - T_\infty$, T is the HGL temperature, T_∞ is the ambient temperature, K_x is a factor to account for the location of the fire within the room, \dot{Q} is the HRR of the fire, ρ_∞ is the density of ambient air, $c_{p,\infty}$ is the specific heat of ambient air, A_o is the area of the vent opening, H_o is the top height of the vent opening, g is the gravitational acceleration, h_w is the effective heat transfer coefficient of the walls, and A_w is the total wall area. The factor K_x is used to correct for whether the chair is in the center of the room ($K_x = 1$), against a wall ($K_x = 1.3$), or in a corner ($K_x = 1.7$). The values of these coefficients are based upon the empirical results of Mowrer and Williamson [29].

The effective heat transfer coefficient is typically modeled by assuming that the walls are thermally thick or thermally thin. The characteristic penetration time of the wall, t_w , is calculated as

$$t_w \equiv \left(\frac{\rho_w c_w}{k_w} \right) \left(\frac{L_w}{2} \right)^2 \quad (4.3)$$

where ρ_w is wall density, c_w is the wall specific heat, k_w is the wall thermal conductivity, and L_w is the thickness of the wall. For times less than t_w , the wall is assumed to be thermally thick, and the effective heat transfer coefficient is computed as

$$h_w = \sqrt{\frac{k_w \rho_w c_w}{t}} \quad (4.4)$$

At times greater than t_w , it is typically assumed that the wall is thermally thin so that $h_w = k_w/L_w$. For standard 1/2 in gypsum wall board with the properties listed in Table 3.3, the penetration time is found to be less than about two minutes. Examination of the chair fires in Fig. 3.1 reveals that the widths of the heat release rate (HRR) peaks at half-height is approximately 3 to 6 minutes. Because of the sharpness of the peaks, though, it is difficult to say whether or not either a thermally thick or a thermally thin approximation is valid. In any case, the MQH simulations presented in Sec. 5 were performed using a switch between thermally thick and thin at the penetration time. This ended up being a conservative estimate, since the times at the peak HRR were in the thermally thin regime for all cases. A thermally thin model will tend to set a lower bound on heat losses from the room, and so the results are conservative with respect to the upper layer temperature—that is, the HGL temperature will tend to be overestimated.

The parameters in Eq. (4.2) may be expressed in terms of the parameters discussed in Sec. 3. The total wall area may be computed as

$$A_w = 2H(\eta_1 + 1) \sqrt{\frac{A_1}{\eta_1}} + 2A_1 - (\mathcal{D}_{12} + \mathcal{D}_{13})H_d W_d \quad (4.5)$$

The vent opening area is the total open door area $A_o = (\mathcal{D}_{12} + \mathcal{D}_{13})H_d W_d$, and the vent opening height is the door height, $H_o = H_d$.

It is straightforward to rearrange the MQH correlation to compute the HRR necessary to achieve a critical temperature rise for flashover. Mathematically, this relationship is

$$\dot{Q}_c = (1.63K_x)^{-3/2} \left(k_w A_w \rho_{\infty} c_{p,\infty} A_o \sqrt{g H_o / L_w T_{\infty}} \right)^{1/2} \Delta T_c^{3/2} \quad (4.6)$$

where it is has been assumed that the walls are thermally thin. The thermally thin assumption follows from the discussion of the previous paragraph, and results in a lower bound estimate for the critical HRR. Equation (4.6) is useful for determining the largest fire that a given room can contain without proceeding to flashover.

There are two approaches for computing the probability of flashover. The most straightforward approach is based on forward MQH model, Eq. (2.3). For the MQH-based loss model the uncertain scenario parameters are $x = \{t_p, \dot{Q}_p, A_1, \eta_1, H, \mathcal{D}, \mathcal{X}\}$, which are used in Eq. (4.2) along with Eq. (4.5) to predict the HGL temperature. Note that the peak HRR, \dot{Q}_p , and the time of the peak HRR, t_p , are dependent on the choice of the fabric combination, a . Using N samples from the

probability distributions for the uncertain parameters in provided in Sec. 3, a set of N temperatures is found using Eq. (4.2). The resultant temperature samples, T_i for $i = 1, \dots, N$ can be used to build a histogram representative of the probability distribution for the uncertain HGL temperature. Additionally, the probability of flashover is obtained by counting the number of temperature samples greater than the flashover temperature and dividing by N . More formally, let $l = 1$ correspond to flashover and $l = 0$ correspond to no flashover. Then the loss model may be expressed as $l = \mathcal{H} [T(x|a) - T_c]$, where $\mathcal{H}(\cdot)$ is the Heaviside step function and $T(x|a)$ is computed using Eq. (4.2). Substitution of this information into Eq. (2.3) gives the equation for computing the probability of flashover for a given fabric combination:

$$\Pr(L = 1|a) = \frac{1}{N} \sum_{i=1}^N \mathcal{H} [T(x_i|a) - T_c] \quad (4.7)$$

An alternative approach for computing the flashover probability is based on the inverse MQH correlation, Eq. (4.6). Beginning with Eq. (2.2) and using the notation of the preceding paragraph gives an alternative equation for computing the probability of flashover

$$\Pr(L = 1|a) = \int_0^\infty d\dot{Q}_p \int dx_0 f_{\dot{Q}_p^*}(\dot{Q}_p|a) f_{X_0}(x_0) \mathcal{H} [\dot{Q}_p - \dot{Q}_c(x_0)] \quad (4.8)$$

where $f_{\dot{Q}_p^*}(\dot{Q}_p|a)$ is the PDF for the peak HRR of chairs with fabric combination a as computed by Eq. (3.2), x_0 is just x excluding the peak HRR parameters, and $f_{X_0}(x_0)$ is the joint probability distribution built from the various probability distributions discussed in Sec. 3. It has been assumed that the walls of the room are thermally thin and so the time of the peak HRR drops out of consideration. It is apparent that the second integral in Eq. (4.8) can be evaluated separately resulting in

$$\Pr(L = 1|a) = \int_0^\infty d\dot{Q}_p f_{\dot{Q}_p^*}(\dot{Q}_p|a) \Pr(\dot{Q}_p \geq \dot{Q}_c) \quad (4.9)$$

This casting of the problem has the advantage that the CDF $\Pr(\dot{Q}_p \geq \dot{Q}_c)$ may be generated using Monte Carlo simulations and then reused for each HRR peak PDF for a given fabric combination. Both Eqs. (4.7) and (4.9) will be used in Sec. 5.

It is important to note that the MQH correlation was derived by fitting data to experiments in which the compartment opened into a large well-ventilated volume. Thus, there was little feedback from the exterior of the fire room. Such scenarios do not correspond exactly with the three room home scenario sketched in Fig. 3.3. The extent of this discrepancy was unknown for typical residential fire scenarios, and so an objective of this research is to develop a quantitative understanding of the difference in predictions from the single-compartment MQH model and the multi-compartment predictions from CFAST.

4.3 Zone Model

Zone models are a class of fire models in which compartments are split into a small number of zones (usually one or two). Within each zone, the state variables are assumed to be constant with respect to spatial location. That is, the thermodynamic state variables are assumed to be lumped with respect to space into a set of average values that are representative of the entire zone. As the

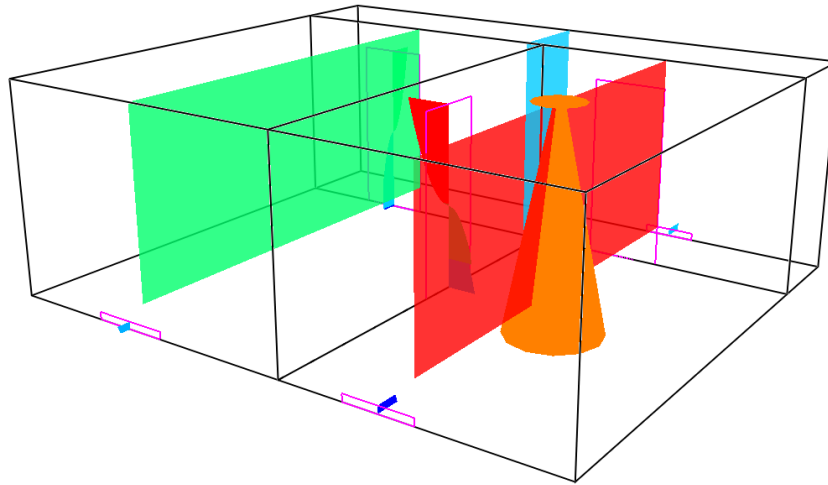


Figure 4.1: Visualization of a typical CFAST simulation.

fire develops, the volume, temperature, and composition of each zone is evolved according to a set of ordinary differential equations derived from conservation of mass and energy principles. In this report, the two-zone Consolidated Model of Fire and Smoke Transport (CFAST) [30] is used to predict the state of the gas throughout the three room structure sketched in Fig. 3.3. CFAST was first released in 1990, but it is based on zone models in development for several years prior. It includes various sub-models and is validated against a significant number of fire experiments [31]. It has been observed that CFAST does tend to over-predict HGL temperature [28], but this is generally a conservative propensity with respect to life safety.

A visualization of a typical CFAST simulation of the generic home is provided in Fig. 4.1. The black lines in Fig. 4.1 represent the edges of compartment walls, and the pink lines are the boundaries of doors or vents. The orange cone-shaped feature represents the fire plume at the peak HRR. The colored rectangles bisecting each room represent the HGL. In this scenario, the HGL in the living room is very close to the floor. The HGL in the bedroom is still relatively hot, but it not quite as low as the living room HGL. The hallway temperature is significantly lower than that in the bedroom because, in this case, the door between the hallway and the living room is closed. Note the vents at the floors in each compartment. These were inserted to account for pressure-induced leakage from the compartments.

There are many advantages of using CFAST for the prediction of fire losses. First, CFAST more accurately models the scenario than empirical correlations. Multiple rooms are allowed, transient heat losses to the walls are taken into account, and the reduction in HRR associated with oxygen depletion is modeled. Second, CFAST provides sufficient information to predict tenability in any of the compartments. In particular, an estimate of thermal FED is possible in addition to HGL temperature-based predictions of flashover. Third, CFAST is relatively efficient. Although much slower than an evaluation of the MQH correlation, CFAST takes orders of magnitude less time than a detailed CFD model. A single run of a typical scenario takes on the order of 3 s on a typical workstation. This makes it possible to run, for instance, 10 000 simulations over the course of a workday.

Table 4.1: Concrete floor thermophysical properties.

Floor Thickness	L_f (m)	0.15
Floor Thermal Conductivity	k_f (W/m·K)	1.75
Floor Density	ρ_f (kg/m ³)	2200
Floor Specific Heat Capacity	c_f (J/kg·K)	1000

Details on the governing equations and implementation of CFAST may be found in the CFAST Technical Reference Guide [30] and so will not be discussed here. However, a few words are appropriate on the model specifics used for the simulations presented in Sec. 5. The floor was assumed to be 0.15 m concrete, and the assumed thermophysical properties are listed in Table 4.1. The assumption of concrete floors is not necessary, and other floor materials are common. Future work should incorporate additional floor materials into the analysis. The walls were chosen to be gypsum with the same properties used in the MQH calculations and listed in Table 3.3.

Another issue that was considered was air leakage from the compartments. This is typically handled in CFAST by creating additional vents areas equal to a typical effective leakage area. Leakage areas are typically quantified as area ratios defined as the equivalent leakage area divided by the total surface area. For typical surfaces, this ratio can range from 10^{-5} to 10^{-2} [32]. For all of the CFAST simulations, a leakage area ratio of 10^{-3} was chosen as appropriate relative to the total compartment surface area. Thus, the equivalent leakage area for room i was computed to be $10^{-3} [2A_i + 2H(L_i + W_i)]$. Leakage was implemented using a 0.08 m high vent at the floor of each compartment where the width was varied to obtain the required effective leakage area.

A couple of assumptions were made concerning the fire. First, the fire was assumed to be at the floor of the compartment. This is a conservative estimate with respect to the HGL temperature. Second, the horizontal area of the base of the fire was assumed to be 0.8 m^2 . This is representative of a typical RUF chair.

Two loss metric were considered: flashover in the living room, and thermally fatal conditions in the bedroom. The first of these loss metrics is a function of HGL temperature in the living room. The flashover probability is calculated using Eq. (4.7) only with an extended uncertain parameter set. Instead of only peak HRR values being used, an entire time-HRR curve, γ , was used—as sampled with Eq. (3.3).

The thermal FED defined in Eq. (4.1) will be used to determine the occurrence of fatal conditions in the bedroom. The integral was approximated using a simple rectangular rule integration of the CFAST outputs at 10 s intervals. The heat flux was computed by defining a CFAST target at the floor of the bedroom. Following Peacock et al. [14], the following algorithm is used for determining which temperature to apply in Eq. (4.1) in terms of the height of the HGL interface, z_l , and the HGL temperature:

- if $z_l > 1.5$ m, use the lower layer temperature;
- if $1 \text{ m} < z_l < 1.5$ m and HGL temperature is greater than $50 \text{ }^\circ\text{C}$, use the lower layer temperature;
- if $1 \text{ m} < z_l < 1.5$ m and HGL temperature is less than $50 \text{ }^\circ\text{C}$, use the HGL temperature; or
- if $z_l < 1$ m, use the HGL temperature.

This algorithm is intended to model the response of a typical occupant to the height and temperature of the HGL. The first case accounts for situations in which the HGL is high enough that most occupants would be able to stay in the cooler air below. The second two cases correspond to scenarios in which a typical occupant would choose to stand upright or squat based on the temperature of the HGL. That is, if the HGL is cool enough (i.e., less than 50 °C), then the occupant would be able to stand. If, however, the HGL temperature is too uncomfortable, most people would choose to squat. Finally, for HGLs descended lower than 1 m, it is assumed that occupants would not be able to avoid exposure to the HGL gases.

Section 5

Results

5.1 Overview

The loss models described in the previous section may be simulated with inputs sampled from the building statistics provided in Sec. 3 to estimate losses in typical residences in the United States. These results allow for a comparison of the effectiveness of the different barrier fabrics used in the chair fire tests performed by the CPSC.

The quality of the loss estimates depends on several factors including the accuracy of the input data, the number of Monte Carlo (MC) simulations performed, and the accuracy of the fire models. The accuracy of the output probability distributions depends on the accuracy of the input probability distributions. The discussion in Sec. 3 is largely a justification for probability distributions used to describe the uncertain building and fire scenario parameters. In all cases in which there was a lack of relevant information, the minimal assumption of a uniform distribution was made. Assuming uniform distributions will result in conservative estimates of the uncertainty in the loss metric, provided that the extent of the bounds is not underestimated. This possible over-prediction in uncertainty is not generally a problem since it is consistent with what is known about the potential fire scenarios. Of greater concern with regards to the input data is the potential that the data used is not truly representative. Again, this is not necessarily a problem in that it means that the estimated loss probabilities are the best that can be predicted based on the information available, but it also means that the results could change significantly if better data become available.

A sufficient number of simulations must be performed in order to sufficiently sample from the input probability space. The variance of a MC approximation decreases as $N^{-1/2}$, but it is unknown *a priori* how many samples are needed to achieve the desired precision. There are various techniques for reducing the number of required samples such as Latin hypercube and importance sampling. In the following, it was found that more advanced sampling techniques were not required. Instead, comparing results with increasing N revealed that convergence was achieved with a reasonable number of samples.

Finally, the quality of the results depends on the model uncertainty. Fortunately, the models used in this report have been well-validated against experimental data. McGrattan et al. [28] compared MQH and CFAST model predictions with experimental data from a number of diverse scenarios. Of particular importance for the analysis of this research are the hot gas layer (HGL) temperature, HGL height, and surface heat flux since these quantities are used to predict flashover

and the thermal fractional effective dose (FED). McGrattan et al. [28] found that MQH over predicts HGL temperature by 17 % on average. Note that this bias percentage was determined from cases in which the compartment was ventilated to a large exterior, and so the uncertainty is not necessarily representative of the fire scenarios considered in this report. Similarly, McGrattan et al. [28] found that CFAST over predicts, on average, the HGL temperature by 20 %, under predicts the HGL height by 5 %, and, and over predicts surface heat fluxes by 5 %. These numbers give an idea of the accuracy of the models, but since they are only average quantities, it is not generally possible to apply them as corrections to the model results. An improvement in existing models, or the development of new models could improve the results presented below.

5.2 Predicting Hazard with the MQH Correlation

The MQH correlation provides a link between the size of a fire and the temperature in the hot gas layer (HGL). As discussed in Sec. 4, the correlation is useful for estimating fire losses both in its forward form, predicting flashover, and its inverse form, predicting the size of a fire resulting in flashover. In this section, both of these forms are applied using the building and fire statistics as inputs.

Sampling and evaluating a single MQH case takes on the order of 0.001 s on a typical desktop workstation. Consequently, it takes about 16 min to perform 1 million MC simulations.

5.2.1 Inverse MQH

The inverse mode of the MQH correlation was used to generate a probability distribution for the critical heat release rate (HRR) required to produce flashover in the range of typical living rooms characterized by the building statistics. Essentially, Eq. (4.6) was simulated N times with each simulation corresponding to a sampled living room. It was first necessary to determine if a sufficient number of samples were taken. This may be investigated by plotting a statistic of the critical HRR, \dot{Q}_c as a function of N . Such a convergence plot is provided for the median value of \dot{Q}_c in Fig. 5.1. It is seen that the variability in the estimate of the median flashover HRR is small after around 100 000 samples. Furthermore, even with only 1 000 samples, a reasonable estimate of the median value of \dot{Q}_c is obtained.

The probability density function (PDF) of \dot{Q}_c is provided in Fig. 5.2. This PDF was generated by a normed histogram of 512 000 MC samples. Four distinct peaks are observed. These peaks are a consequence of the discretely distributed building parameters—namely, the fire location and the door opening combination. Fires smaller than 0.5 MW are seen to have a very low probability of causing flashover in the living room, assuming that no other fuel sources become involved. The lower bound of this data is 440 kW implying that, within the uncertainty of the building statistics and the model, fires that remain smaller than this value will not flashover any living room in an ensemble of rooms sampled from the building parameter probability distributions. The 5th percentile of this data is 510 kW. That is, fires smaller than 510 kW will flashover 5 % of living rooms sampled from the input probability distributions. The median critical HRR is 850 kW as seen in Fig. 5.2.

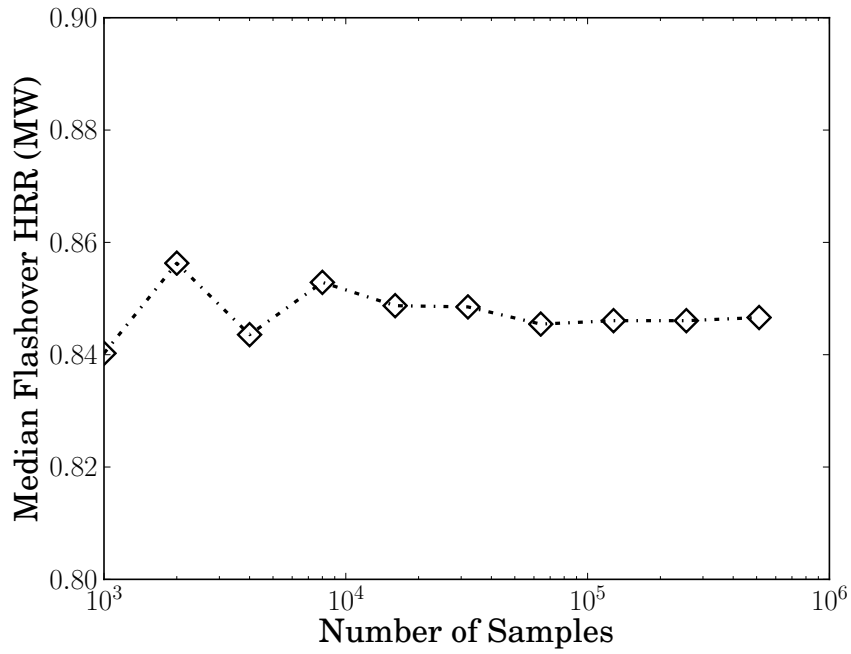


Figure 5.1: Median flashover HRR, as computed by the inverse MQH correlation, versus number of samples.

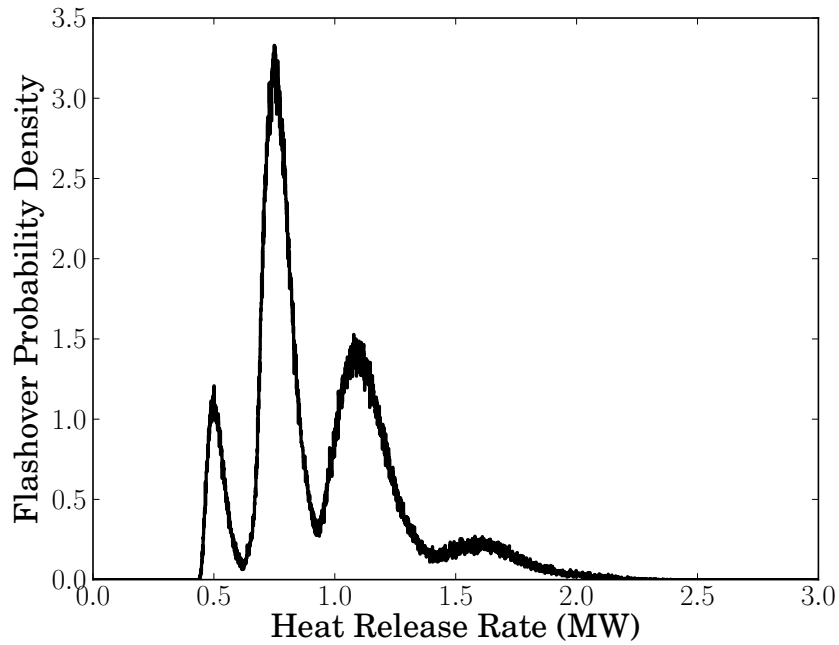


Figure 5.2: Probability density function (PDF) of the critical flashover HRR obtained using the inverse MQH correlation.

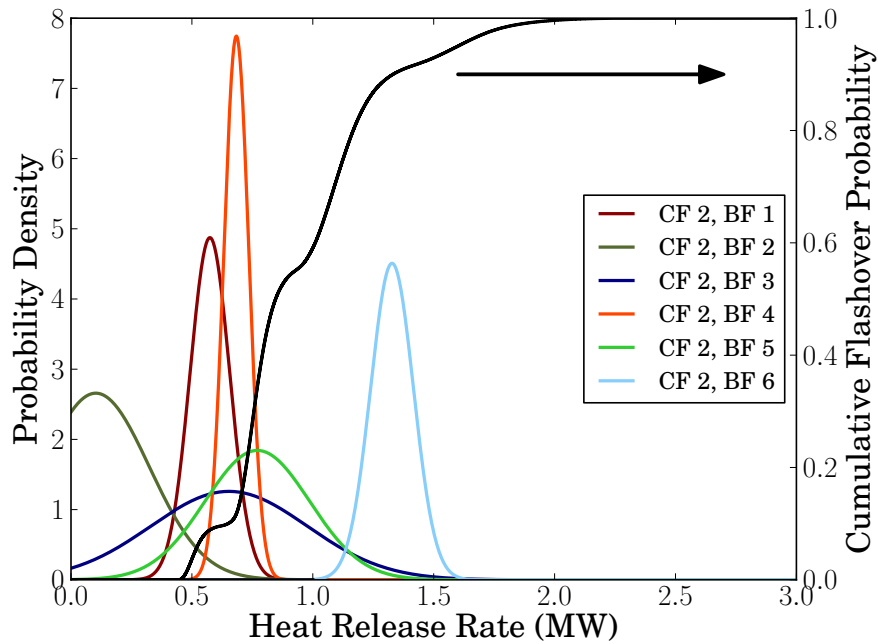


Figure 5.3: Heat release rate PDFs for cover fabric two compared to flashover probability for chairs.

In addition to helping quantify a critical HRR for flashover, the inverse MQH correlation, Eq. (4.6), may also be used to estimate flashover probabilities. This is accomplished using the flashover probability distribution plotted in Fig. 5.2 as a cumulative distribution function (CDF), $\Pr(\dot{Q}_p \geq \dot{Q}_c)$. The CDF is substituted into Eq. (4.9) along with the peak HRR PDF in the form of Eq. (3.2). Both the CDF and peak HRR PDFs for the RUF fires with cover fabric two are plotted in Fig. 5.3. An equivalent plot for cover fabric three is provided in Fig. 5.4. The degree to which the colored PDFs overlap with the CDF (black line) corresponds to the probability of flashover. As was noted in Sec. 3, cover fabric three tends to produce more intense fires. Thus the peak HRR PDFs in Fig. 5.4 overlap with the critical HRR CDF to a greater extent than those in Fig. 5.3, and thus chairs wrapped with cover fabric three are more likely to result in flashover of the living room. Similarly, barrier fabric six is seen to produce a much greater likelihood of flashover according to the MQH correlation.

The probabilities of flashover for the various fabric combinations computed using the inverse MQH correlation and 512 000 samples from the building data probability distributions are provided in Table 5.1. These values were computed using Eq. (4.9). Evaluation of Eq. (4.9) may be visualized with the aid of Figs. 5.3 and 5.4. The flashover probability is computed as the integrated product of the colored lines with the black line. As previously mentioned, cover fabric three and barrier fabric six are the most likely to cause flashover. Barrier fabric two is seen to reduce the flashover probability to less than 1 % if used with cover fabric two. On the other end of the severity spectrum, chairs with barrier fabric six are, on average, more than 90 % likely to lead to flashover of living rooms.

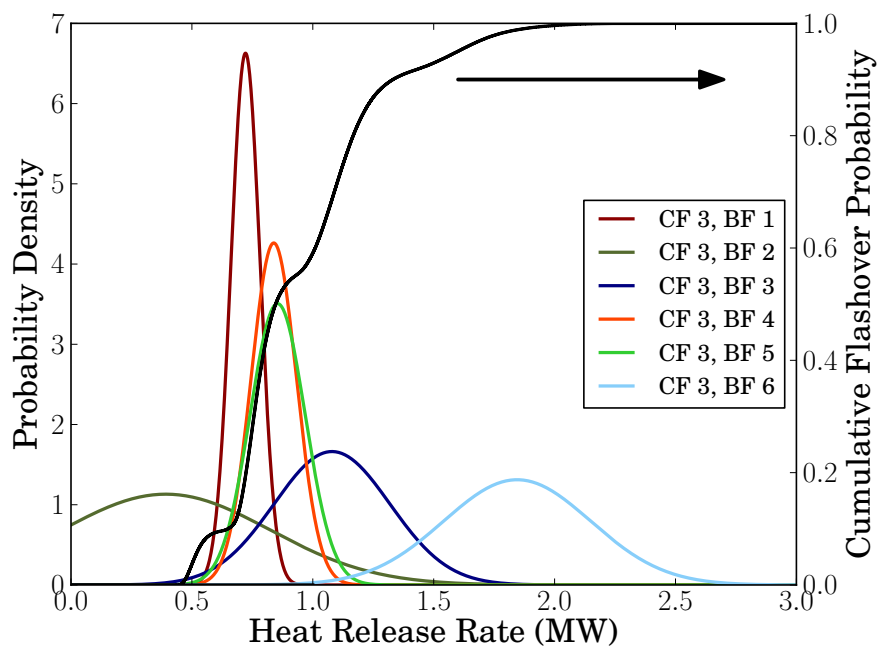


Figure 5.4: Heat release rate PDFs for cover fabric three compared to flashover probability for chairs.

Table 5.1: Flashover probabilities of all fabric combinations using the inverse MQH method.

Cover Fabric	Barrier Fabric	Flashover Probability
2	1	8.2 %
2	2	0.6 %
2	3	26.5 %
2	4	15.6 %
2	5	33.8 %
2	6	88.9 %
3	1	22.8 %
3	2	17.4 %
3	3	66.2 %
3	4	43.6 %
3	5	44.8 %
3	6	97.0 %

5.2.2 Forward MQH

The results of the previous section provide useful information on the allowable size of RUF fires in a statistical ensemble of rooms that is to some extent representative of living rooms across the United States. The inverse MQH correlation does not provide information about the HGL temperature, however. In this section, the forward MQH correlation is used to predict a distribution HGL temperatures, which is in turn used to compute flashover probabilities. This approach is equivalent with the approach taken using the CFAST model in the next section. Also, in contrast to the previous section, the flashover probability calculations will be based on a discrete distribution of peak HRR values so the estimates will be slightly different than those of Table 5.1. Specifically, peak HRR values will be sampled using Eq. (3.1) rather than Eq. (3.2). It is of interest to see how much of an effect this choice of models has on the predicted flashover probabilities.

The basic approach is to generate samples of living room parameters from the probability distributions of Sec. 3 and then use these samples to compute an ensemble of HGL temperatures for the different fabric combinations. A plot of the CDFs of the peak living room HGL temperature grouped by barrier fabric is shown in Fig. 5.5. These CDFs were created as normed histograms of 131 584 samples for each fabric combination. After the grouping by barrier fabric, each CDF in Fig. 5.5 is based on 263 168 samples. The vertical dotted line at 522 °C represents the assumed value of the flashover temperature. The point at which the CDF curves intersect this critical line correspond to the flashover probability. There is a greater than 60 % probability that chairs with barrier fabric two will not result in HGL temperatures greater than about 10 °C higher than the ambient temperature of 22 °C. This is due to the fact that a number of the chairs with barrier fabric two did not ignite. On the other hand, there are almost no chairs with barrier fabric six that do not result in a HGL temperature exceeding 400 °C. The four remaining barrier fabrics result in peak HGL living room temperatures distributed between these two extremes.

It is also helpful to look at the distribution of temperatures with respect to the two cover fabrics. A plot of the living room temperature CDFs for cover fabrics two and three is shown in Fig. 5.6. Each of these CDFs is a normed histogram generated from 789 504 samples after combining the samples from each of the six barrier fabrics combined with the corresponding cover fabric. It is apparent that the choice of cover fabric has much less influence on the potential for flashover than does the choice of barrier fabric—at least for those materials considered in this report. The change in flashover probability between the two cover fabrics is about 20 % as compared to about 90 % for the change between barrier fabric 2 and barrier fabric 6 as seen in Fig. 5.5.

As with the inverse MQH simulations discussed in the previous section, the convergence of the simulations was checked by plotting the flashover probability versus the number of samples for each fabric combination in Fig. 5.7. As with the inverse MQH simulations, the flashover probabilities vary little after around 100 000 samples. Also, it is observed that fairly accurate estimates of the flashover probabilities is obtained with even around 1000 samples.

The flashover probabilities computed using the forward MQH correlation and the discrete distribution for the HRR peaks are compiled in Table 5.2. There is little difference with the values in Table 5.1. The greatest difference in terms of probabilities is for the cover fabric two, barrier fabric five combination in which the probability of flashover is 3.4 % higher for the inverse MQH

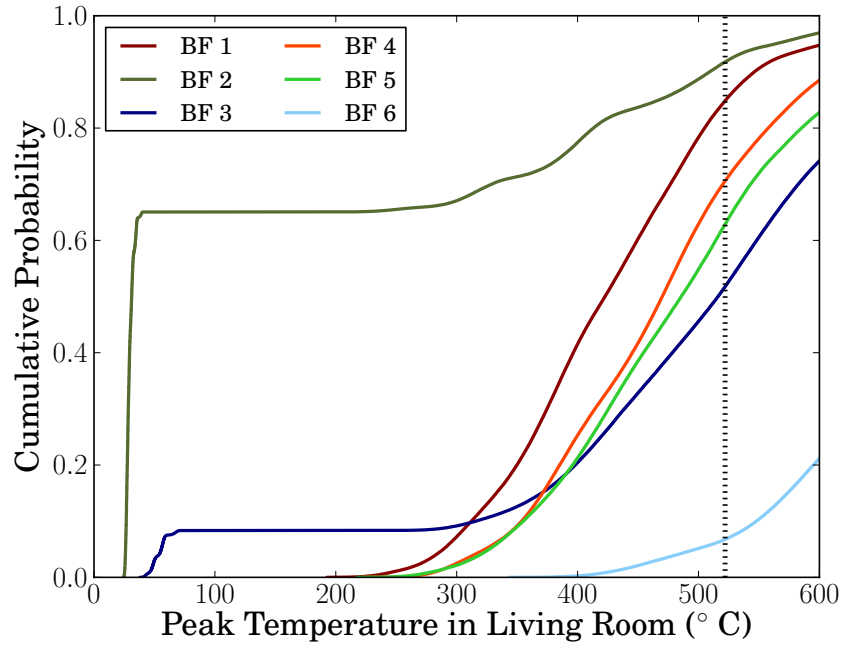


Figure 5.5: Cumulative probability distribution for hot gas layer temperature in living room for all barrier fabrics as predicted by the MQH correlation.

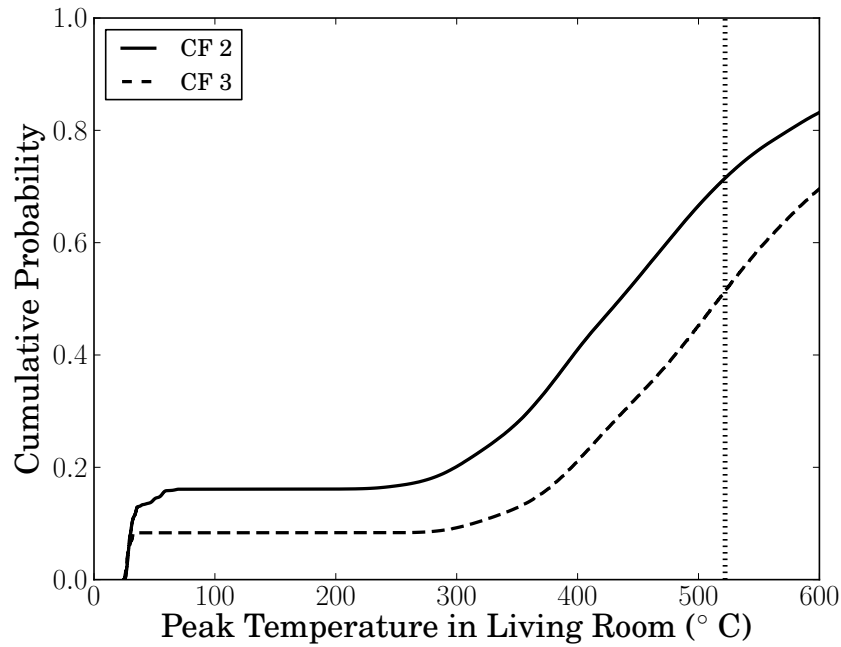


Figure 5.6: Cumulative probability distribution for hot gas layer temperature in living room for both cover fabrics as predicted by the MQH correlation.

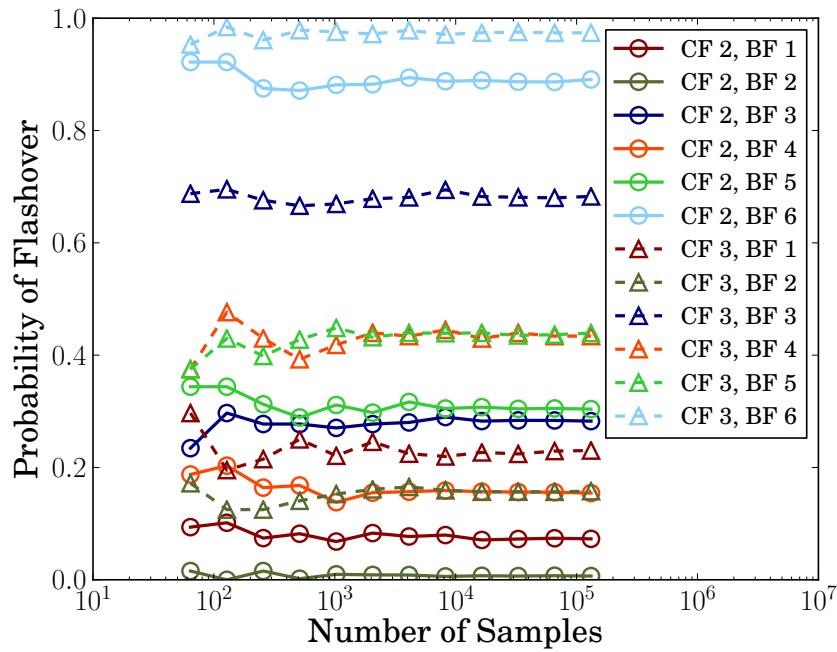


Figure 5.7: Convergence of flashover probabilities using MQH based model.

Table 5.2: Flashover probabilities of all fabric combinations using MQH based model.

Cover Fabric	Barrier Fabric	Flashover Probability
2	1	7 %
2	2	1 %
2	3	28 %
2	4	15 %
2	5	30 %
2	6	89 %
3	1	23 %
3	2	16 %
3	3	68 %
3	4	43 %
3	5	44 %
3	6	97 %

calculation. This discrepancy is due to the fact that the PDF for that fabric combination straddles the rapidly increasing region of the critical flashover CDF. Thus, small variations in the probability distribution for the cover fabric 2, barrier fabric 5 combination will result in large variations in the flashover probability.

It is helpful to group the flashover probabilities in terms of the barrier fabrics since the objective of this report is to assess the impact that barrier fabrics have on RUF fire hazard. The probabilities

Table 5.3: Flashover probabilities from barrier fabrics using forward MQH model.

Barrier Fabric	Flashover Probability
1	15 %
2	8 %
3	48 %
4	29 %
5	37 %
6	93 %

that a chair with one of the six barrier fabrics will cause a living room to flashover are listed in Table 5.3. The effectiveness of several of the barrier fabrics in reducing the flashover probability is clear. Compared with the worst performing barrier fabric (barrier fabric six), all of the other barriers have reduce the flashover probability by at least about 45 %. The best performing barrier fabric reduces the flashover risk to only 8.2 %.

The MQH results show a clear distinction in the performance of the several barrier fabrics. These results are limited for several reasons, though. The only loss metric considered is the transition to flashover. Therefore, it is impossible to make any predictions concerning life safety in adjoining rooms. Perhaps of greater importance, however, is that the MQH correlation is based on data for compartments venting to an arbitrarily large exterior. Because of this, it is likely that the flashover probabilities will be over-predicted. In the next section, similar simulations are performed using CFAST as the fire model. The CFAST results will not be subject to these limitations.

5.3 Predicting Hazard with CFAST

Hazardous conditions in both the living room and the bedroom were estimated for all 12 fabric combinations using CFAST. Specifically, transition to flashover and the thermal FED were computed. Up to 10 000 MC simulations for each fabric combination were performed. A typical CFAST scenario took approximately 3 s of CPU time on a typical desktop workstation.

It was found that for almost all of the fabric combinations, the RUF chair fires were insufficiently large to flashover the living room. The only exception was for chairs covered with cover fabric three and barrier fabric six. These chairs had only a 0.1 % chance of causing flashover. The discrepancy between this result and that obtained using the MQH correlation is due to the previously mentioned fact that the MQH correlation was developed using data in which the compartment vents were connected to a large open space rather than an adjacent compartment. It was observed that the HGL temperatures in CFAST were considerably lower for cases in which the door openings were defined to be connected to the exterior of the home rather than to the adjacent bedroom and hallway. It was observed that for otherwise identical cases, the peak HRR was almost halved in scenarios in which the living room doors opened to the other interior rooms. This decrease in HRR was seen to correspond to a near halving in the available oxygen in the living room.

Since the flashover probabilities were all effectively zero, convergence of the simulations were checked by considering another statistic—namely, the probability that the bedroom thermal FED

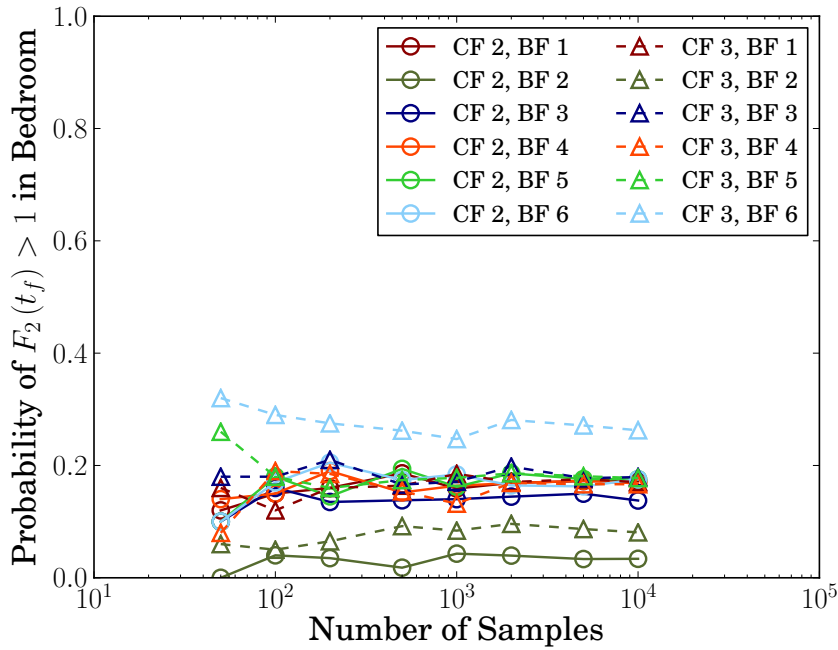


Figure 5.8: Convergence of the probability of the living room fractional effective dose exceeding one.

exceeded one at any point in the simulation time. A thermal FED greater than one corresponds to lethal conditions for 50 % of the population in the bedroom. A plot of the probability of lethal conditions in the bedroom versus the number of MC simulations is shown in Fig. 5.8. It appears that the variability in the failure probability is small for results based on more than 2 000 simulations. More simulations could be performed to confirm this, but it would take approximately 42 CPU days to run 100 000 simulations for each of the 12 fabric combinations. Such a calculations would be possible utilizing multiple processors, but the variability apparent in Fig. 5.8 is sufficiently small that such an effort is not necessary.

The probabilities that the final thermal FED in the bedroom, $F_2(t_f)$ exceeds one are listed in Table 5.4 for each of the six barrier fabrics. Note that these probabilities correspond to 20 000 simulations for each barrier fabric. Clearly, none of the barrier fabrics completely eliminate the hazard in the bedroom. However, a substantial reduction in hazard is seen between barrier fabrics six and two. The remaining four barrier fabrics are seen to have intermediate and relatively similar hazard potential for occupants in the bedroom.

More information on the bedroom thermal FED is presented in Fig. 5.9 in which the full CDFs for each barrier fabric are plotted. For all cases, there is a probability of at least about 20 % that the bedroom thermal FED is effectively zero. These cases of near zero thermal FED correspond to scenarios in which the bedroom is not connected to the living room because the doors are closed. The thermal FED is never exactly zero since the integral written in Eq. (4.1) is always nonzero. Barrier fabric two has about a 70 % probability of the FED being approximately zero as

Table 5.4: Probability of lethal condition in the bedroom for each barrier fabric base on the thermal FED.

Barrier Fabric	Probability of FED > 1
1	17 %
2	6 %
3	16 %
4	17 %
5	18 %
6	22 %

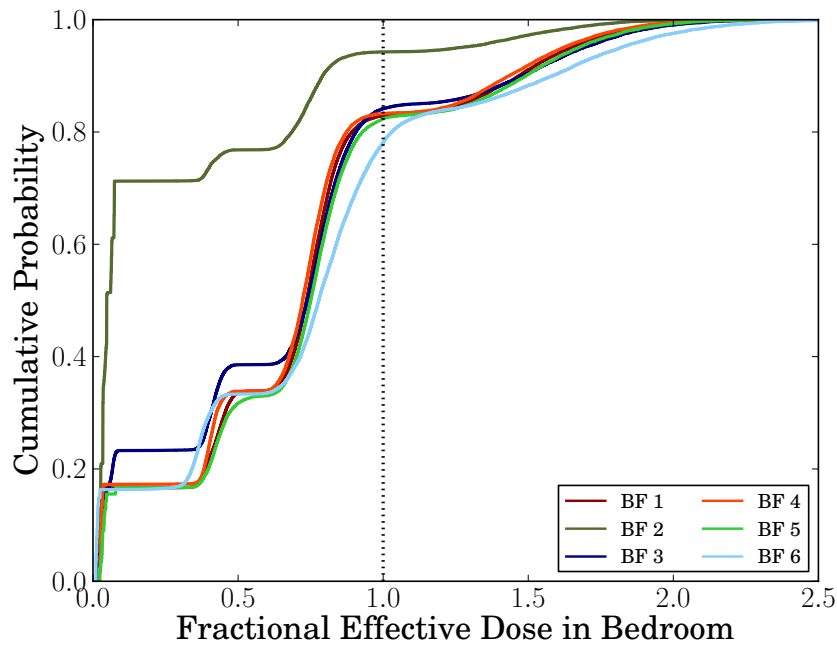


Figure 5.9: Cumulative distribution function for bedroom thermal FED in bedroom for all barrier fabrics as predicted using CFAST.

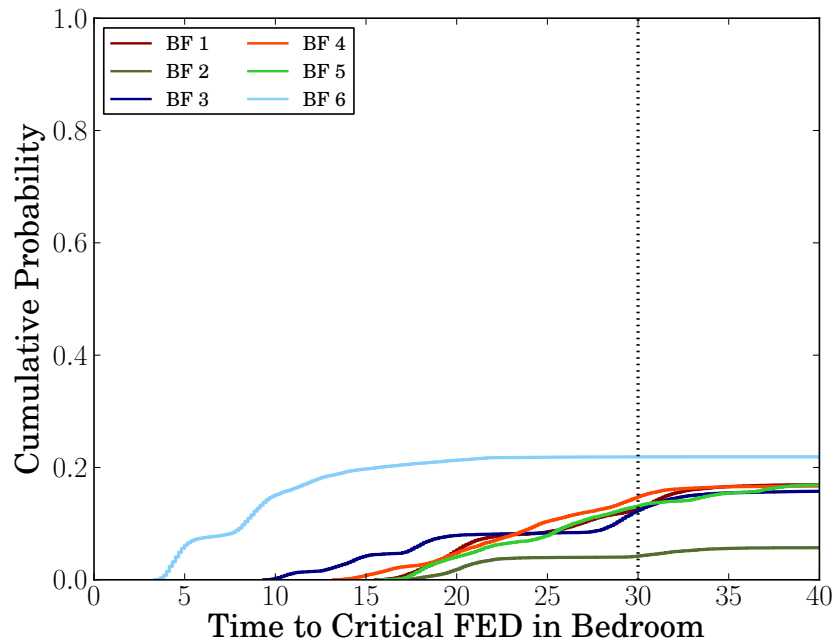


Figure 5.10: Cumulative distribution function for the time at which the bedroom thermal FED exceeds one for all barrier fabrics as predicted using CFAST.

a consequence of the cases in which the chairs with barrier fabric two fail to burn.

As is apparent from Fig. 3.1, the different fabric combinations affect not only the peak HRR, but also the time at which that peak is reached. It is therefore, appropriate to investigate the time at which the critical FED is reached by the various barrier fabrics. A plot of such information is given in Fig. 5.10. Note that for barrier fabric six, thermal hazard in the bedroom becomes a strong possibility at around five minutes. By comparison other barrier fabrics are seen to delay the time to the critical thermal FED until 10 to 20 min after ignition. A particular time may be examined such as 30 min as is represented by the dotted vertical line in Fig. 5.10. At this time, the intermediately performing barrier fabrics are seen to represent a significant advantage over barrier fabric six as the probability of lethal conditions is nearly halved for all cases.

Note that the assumption of the residential layout as shown in Fig. 3.3 might have an influence on the results obtained here. In particular, for scenarios in which the home section of Fig. 3.3 is ventilated to additional rooms, it is likely that the bedroom conditions will not be as severe. Additional rooms were not included in the analysis for the reasons provided in Sec. 3, but future analysis should consider the sensitivity of these results to that assumption.

The conditions in the bedroom have been discussed first since it was observed that flashover is highly unlikely for all of the chair fires. However, for completeness, the temperature and thermal FED in the living room will be described. A plot of the HGL temperature CDF for the living room is provided in Fig. 5.11. Although the chair fires are too small to flashover the compartment for in almost all scenarios, a significant difference in performance is observed. Because chairs with barrier fabric two do not burn in many cases, there is about a 65 % probability that the

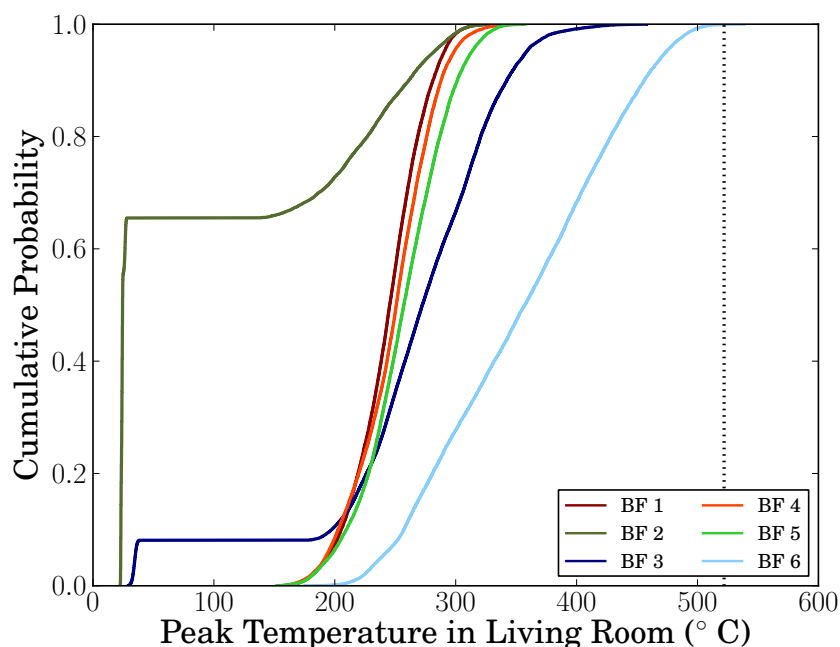


Figure 5.11: Cumulative distribution function for HGL temperature in living room for all barrier fabrics as predicted using CFAST.

room temperature remains ambient for chairs wrapped in barrier fabric two. Furthermore, with the exception of barrier fabrics three and six, there is a greater than 80 % probability that the temperature does not exceed 300 °C in the living room. Such an HGL temperature is certainly hazardous in the living room, but it also corresponds to significantly safer conditions in other parts of the home.

It is helpful to examine the correlations between the various loss metrics. First, focusing on the living room, a scatter plot of living room thermal FED versus living room peak HGL temperature is given in Fig. 5.12. The 120 000 markers in Fig. 5.12 each correspond to a single CFAST simulation. The dotted lines represent critical the values of temperature and FED. Although the living room will not flashover given the chair fires considered, it will almost always be untenable. Only a few cases are thermally tenable because several of the ignited chairs self-extinguish before the polyurethane foam padding becomes involved. Since the thermal FED is largely a function of HGL temperature, there is a clear correlation in the scatter plot.

The correlation between the bedroom FED and the living room HGL temperature is plotted in Fig. 5.14. In this case, as was seen in Fig. 5.9, the majority of scenarios are not lethal for bedroom occupants. It is interesting to note the four distinct groupings of the data in Fig. 5.9. Each of these corresponds to a distinct door opening combination, \mathcal{D} . The group of markers with the lowest values of thermal FED corresponds to cases in which there is no ventilation path between the bedroom and the living room—that is, all of the doors to the bedroom are closed. The second lowest group of markers is associated with scenarios in which the hot gases pass down the hallway to bedroom. The third highest group, in which the thermal FED values are close to one, is due to

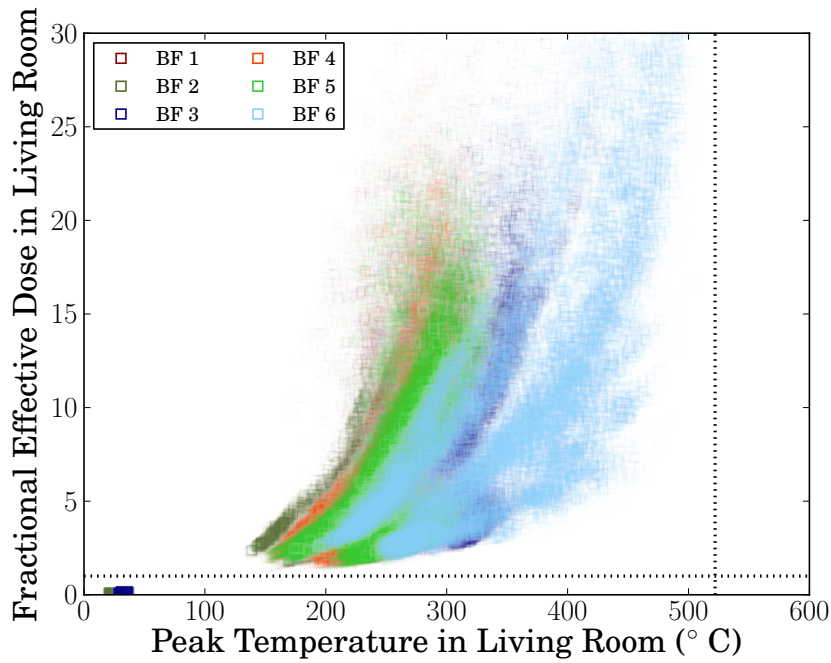


Figure 5.12: Scatter plot of living room fractional effective dose versus living room hot gas layer temperature computed using CFAST with 10 000 samples for each barrier fabric.

the scenarios in which hot gases escape to both the bedroom and the hallway. The final, and most severe, grouping of scenarios corresponds to those cases in which the hot gases move directly and exclusively from the living room to the bedroom.

The data in Fig. 5.9 may be summarized in terms of means and standard deviations. This reduced statistical picture of the data is plotted in Fig. 5.14. The standard deviations are a result of both the uncertainty in the RUF chair fire experiments as well as the uncertainty in the building scenario parameters. It is observed that the average final thermal FED in the bedroom is not much larger for barrier fabric six than it is for barrier fabrics one, three, four, and five. The relatively good performance of barrier fabric two is demonstrated once again.

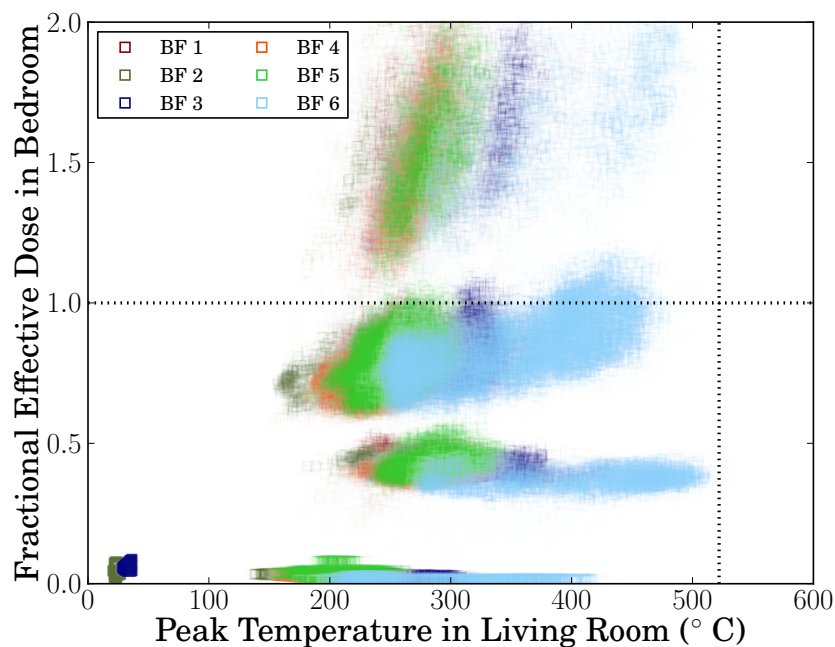


Figure 5.13: Scatter plot of bedroom fractional effective dose versus living room hot gas layer temperature computed using CFAST with 10 000 samples for each barrier fabric.

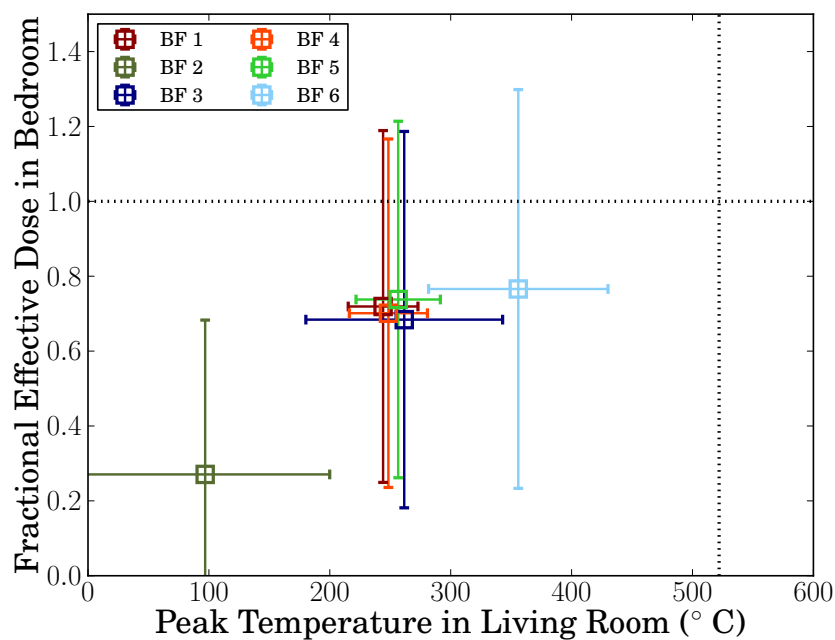


Figure 5.14: Bedroom fractional effective dose versus living room hot gas layer temperature average values computed using CFAST with 10 000 samples for each barrier fabric. The error bars represent one standard deviation.

Section 6

Conclusions

The potential for barrier fabrics to reduce the flammability of residential upholstered furniture (RUF) is being considered by the Consumer Product Safety Commission (CPSC). In order to investigate the effectiveness of barrier fabrics at improving life safety in RUF fires, a probabilistic methodology for estimating fire losses was developed. This methodology is based on Monte Carlo (MC) simulations of fire models. As this report is the first presentation of this methodology, the implementation is still in prototype form. The focus has been on the building statistical data and the theory underlying the approach.

The probabilistic method for estimating fire losses requires a statistical description of the fire scenarios. Such a statistical description was developed from relevant census, code, and survey data. Concurrently, a statistical description of RUF chair fires with different fabric combinations was derived from data provided by the CPSC. The probability distributions describing these scenario parameters may be used to generate an ensemble of residential fire scenarios that is to some degree representative of home fires in the United States.

Two models were used to perform the MC simulations. The first model was the MQH correlation for predicting hot gas layer (HGL) temperature as a function of heat release rate (HRR). The HGL temperature was used as a criterion flashover. While the MQH correlation predicted a significant number of living room flashovers for all fabric combinations and room scenarios in the statistical ensemble sampled, similar calculations using the zone model CFAST indicate that flashover from a single chair is very unlikely for the chairs and floor plan considered. The CFAST model indicates that even though flashover is unlikely in the living room, that lethal conditions may be possible in both the living room and an adjacent bedroom. Lethal conditions were characterized in terms of a thermal fractional effective dose (FED).

A clear distinction between barrier fabrics was observed. Use of the worst barrier fabric resulted in significantly higher temperatures and thermal FEDs in all rooms considered. One of the barrier fabrics consistently performed better than the rest. In many cases this barrier fabric protected the chair from burning, and conditions were safe throughout the structure. The four intermediately performing barrier fabrics provided a significant reduction in HGL temperature in the living room when compared to the worst performing barrier fabric. In terms of the thermal FED, however, the intermediate barriers provided only a marginal improvement over the worst barrier. This is due to the fact that thermal FED is defined as an integrated quantity, and even though the intermediate barriers reduced the peak HRR, they tended to burn for longer periods of time thus steadily increasing the thermal FED. It is unclear if the thermal FED is appropriate for these long time scales.

In any case, the intermediate barriers did tend to delay the time at which a critical thermal FED was reached. In order to quantify the advantage of this delay, it will be necessary to include some analysis of occupant egress in residential scenarios.

The research described in this report has many paths for future development. The MC methodology produces a large amount of data, and it is possible to extract additional useful information from these results. In particular, sensitivity analysis of the uncertain parameters may be easily investigated by producing scatter plots of predicted loss metrics versus the various uncertain parameters. Such plots will allow for identification of those scenario parameters which are most influential on life safety. Those parameters found to be uninfluential do not need to be better characterized or even varied in future simulations. Conversely, those parameters seen to have a significant impact on the loss metrics should be better characterized in terms of their probability distributions. In addition to a deeper analysis of the available data, details should be added to the CFAST model. Specifically, it is important to investigate the hazard consequences of larger RUF fires since those considered in this report did not result in flashover in nearly all of the cases considered. Similarly, the addition of secondary RUF fires into the model will result in more realistic and severe scenarios. It is likely that the consideration of more severe fire scenarios will allow for a more precise differentiation of the fabric combinations under consideration. It was noted that the home model given in Fig. 3.3 might have some limitations due to the lack of fresh air from the rest of the home. The effects of this assumption should be studied by including a door from the hallway to an additional large room to represent the rest of the house or possibly just a door opening to the home exterior. A very practical piece of future work is to use the CFAST model, coupled to a well-chosen set of design fires to identify a critical HRR as was done with the MQH correlation. Future model developments should include the addition of smoke alarms and some consideration of reasonable egress times for building occupants. The limitations of the CFAST model should be explored through the use of more detailed simulations using the Fire Dynamics Simulator (FDS) [33]. The sensitivity of the results to the response of occupants to the HGL height and temperature should be studied. Finally, the methodology could be used to quantify reductions in civilian deaths by focusing on the scenarios in which most fatalities occur according to the fire statistics.

References

- [1] M. Ahrens. Home structure fires. Technical Report USS12G, National Fire Protection Association, Quincy, Massachusetts, 2015.
- [2] J.R. Hall. Estimating fires when a product is the primary fuel but not the first fuel, with an application to upholstered furniture. *Fire Technology*, 51:381–391, 2015.
- [3] R.G. Gann, V. Babrauskas, and R.D. Peacock. Fire conditions for smoke toxicity measurement. *Fire and Materials*, 18:193–199, 1994.
- [4] R.W. Bukowski. Evaluation of furniture-fire hazard using a hazard-assessment computer model. *Fire and Materials*, 9(4):159–166, 1985.
- [5] R.D. Peacock and R.W. Bukowski. A prototype methodology for fire hazard analysis. *Fire Technology*, 26:15–40, 1990.
- [6] F.B. Clarke, R.W. Bukowski, R.W. Steifel, J.R. Hall, and S.A. Steele. The National Fire Risk Assessment Project—Final Report. Technical report, National Fire Protection Research Foundation, Quincy, Massachusetts, 1990.
- [7] R.W. Bukowski, F.B. Clarke, J.R. Hall, and R.W. Steifel. The National Fire Risk Assessment Project—Case Study 1: Upholstered Furniture in Residences. Technical report, National Fire Protection Research Foundation, Quincy, Massachusetts, 1990.
- [8] V. Babrauskas. Fire hazard and upholstered furniture. In *Third European Conference on Furniture Flammability*, pages 125–133, Brussels, 1992. Interscience Communications Ltd.
- [9] R.D. Peacock, P.A. Reneke, R.W. Bukowski, and V. Babrauskas. Defining flashover for fire hazard calculations. *Fire Safety Journal*, 32:331–345, 1999.
- [10] P.H. Thomas. Testing products and materials for their contribution to flashover in rooms. *Fire and Materials*, 5(3):103–111, 1981.
- [11] B.J. McCaffrey, J.G. Quintiere, and M.F. Harkleroad. Estimating room fire temperatures and the likelihood of flashover using fire test data correlations. *Fire Technology*, 17:98–119, 1981.
- [12] V. Babruaskas, R.D. Peacock, and P.A. Reneke. Defining flashover for fire hazard calculations: Part ii. *Fire Safety Journal*, 38:613–622, 2003.

- [13] T.J. Ohlemiller and R.G. Gann. Estimating reduced fire risk resulting from an improved mattress flammability standard. Technical Note 1446, National Institute of Standards and Technology, Gaithersburg, Maryland, 2002.
- [14] R.D. Peacock, J.D. Averill, P.A. Reneke, and W.W. Jones. Characteristics of fire scenarios in which sublethal effects of smoke are important. *Fire Technology*, 40:127–147, 2004.
- [15] International Organization for Standardization (ISO). *ISO 13571, Life-threatening components of fire—Guidelines for the estimation of time available for escape using fire data*.
- [16] R.R. Upadhyay and O.A. Ezekoye. Treatment of design fire uncertainty using quadrature method of moments. *Fire Safety Journal*, 43:127–139, 2008.
- [17] D. Kong, N. Johansson, S. Lu, and S. Lo. A monte carlo analysis of the heat release rate uncertainty on available safe egress time. *Journal of Fire Protection Engineering*, 23:5–29, 2012.
- [18] B. Sundström, Research Commission of the European Communities. Directorate-General for Science, Development, Commission of the European Communities, European Commission Measurement, and Testing Programme. *CBUF: Fire Safety of Upholstered Furniture : the Final Report on the CBUF Research Programme*. EUR (Series). European Commission Measurements and Testing, 1995.
- [19] V. Babrauskas. Upholstered furniture room fires—measurements, comparison with furniture calorimeter data, and flashover predictions. *Journal of Fire Sciences*, 2:5–19, 1984.
- [20] International Code Council, Inc. *International Residential Code*.
- [21] K. Ghazi Wakili, E. Hugi, L. Wullschleger, and T. Frank. Gypsum board in fire—modeling and experimental validation. *Journal of Fire Sciences*, 25:267–282, 2007.
- [22] U.S. Census Bureau, Suitland, Maryland. *American Housing Survey for the United States: 2013*, 2013.
- [23] Paul Emrath. Spaces in new homes. Technical report, National Association of Home Builders (NAHB), 2013.
- [24] U.S. Energy Information Administration, Washington, District of Columbia. *Residential Energy Consumption Survey*, 2009.
- [25] Eric Jones, Travis Oliphant, Pearu Peterson, et al. SciPy: Open source scientific tools for Python, 2001–. [Online; accessed 2016-03-01].
- [26] D.A. Purser. *SFPE Handbook of Fire Protection Engineering*, chapter Assessment of Hazards to Occupants from Smoke, Toxic Gases, and Heat. National Fire Protection Association, Quincy, Massachusetts, 4th edition, 2008.
- [27] W.D. Walton and P.H. Thomas. *SFPE Handbook of Fire Protection Engineering*, chapter Estimating Temperatures in Compartment Fires. National Fire Protection Association, Quincy, Massachusetts, 4th edition, 2008.

- [28] K. McGrattan, R. Peacock, and K. Overholt. Validation of fire models applied to nuclear power plant safety. *Fire Technology*, 52:5–24, 2016.
- [29] F.W. Mowrer and R.B. Williamson. Estimating room temperatures from fires along walls and in corners. *Fire Technology*, 23:133–145, 1987.
- [30] R. D. Peacock, K.B. McGrattan, G. P. Forney, and P. A. Reneke. CFAST – Consolidated Model of Fire Growth and Smoke Transport (Version 7) Volume 1: Technical Reference Guide. Technical Note 1889v1, National Institute of Standards and Technology, Gaithersburg, Maryland, 2016.
- [31] R. D. Peacock, G. P. Forney, and P. A. Reneke. CFAST – Consolidated Model of Fire Growth and Smoke Transport (Version 7) Volume 3: Verification and Validation Guide. Technical Note 1889v3, National Institute of Standards and Technology, Gaithersburg, Maryland, 2016.
- [32] National Fire Protection Association, Quincy, Massachusetts. *NFPA 92, Standard for Smoke Control Systems*, 2012.
- [33] K. McGrattan, S. Hostikka, R. McDermott, J. Floyd, C. Weinschenk, and K. Overholt. Fire dynamics simulator, technical reference guide volume 1: Mathematical model. Technical report, NIST, 2015.